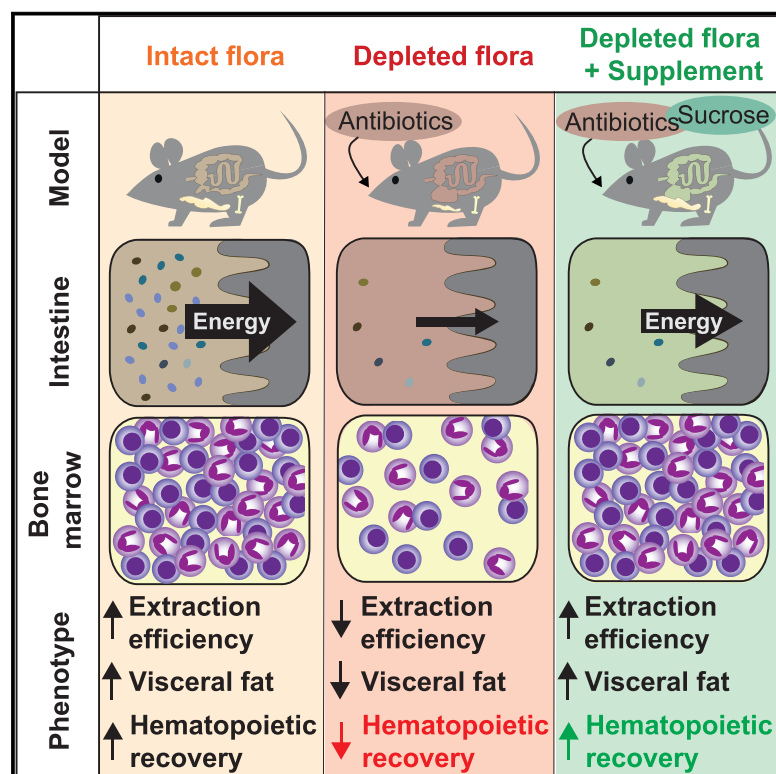


# Cell Host & Microbe

## Nutritional Support from the Intestinal Microbiota Improves Hematopoietic Reconstitution after Bone Marrow Transplantation in Mice

### Graphical Abstract



### Authors

Anna Staffas, Marina Burgos da Silva, Ann E. Slingerland, ..., David E. Cohen, Robert R. Jenq, Marcel R.M. van den Brink

### Correspondence

vandenbm@mskcc.org

### In Brief

Intestinal bacteria can exert effects on systemic hematopoiesis. Staffas et al. show that the intestinal flora contributes to hematopoietic recovery after bone marrow transplantation (BMT) through improved dietary energy uptake. The findings suggest possible clinical intervention strategies for improved BMT outcomes.

### Highlights

- Intestinal microbiota depletion impairs hematopoiesis after bone marrow transplantation
- Intestinal flora depletion decreases energy harvest and reduces visceral adipose tissue
- Caloric supplementation rescues impaired hematopoiesis in microbiota-depleted mice
- The effects of intestinal flora disruption are dose dependent



# Nutritional Support from the Intestinal Microbiota Improves Hematopoietic Reconstitution after Bone Marrow Transplantation in Mice

Anna Staffas,<sup>1</sup> Marina Burgos da Silva,<sup>1</sup> Ann E. Slingerland,<sup>1</sup> Amina Lazrak,<sup>1</sup> Curtis J. Bare,<sup>2</sup> Corey D. Holman,<sup>2</sup> Melissa D. Docampo,<sup>1,3</sup> Yusuke Shono,<sup>1</sup> Benjamin Durham,<sup>4</sup> Amanda J. Pickard,<sup>5</sup> Justin R. Cross,<sup>5</sup> Christoph Stein-Thoeringer,<sup>1</sup> Enrico Velardi,<sup>1</sup> Jennifer J. Tsai,<sup>1</sup> Lorenz Jahn,<sup>1</sup> Hillary Jay,<sup>1</sup> Sophie Lieberman,<sup>1</sup> Odette M. Smith,<sup>1</sup> Eric G. Pamer,<sup>1,6,7,8</sup> Jonathan U. Peled,<sup>1,6,9</sup> David E. Cohen,<sup>2</sup> Robert R. Jenq,<sup>10</sup> and Marcel R.M. van den Brink<sup>1,6,9,11,\*</sup>

<sup>1</sup>Department of Immunology, Sloan Kettering Institute, Memorial Sloan Kettering Cancer Center, New York, NY 10065, USA

<sup>2</sup>Joan and Sanford I. Weill Department of Medicine, Division of Gastroenterology and Hepatology, Weill Cornell Medical College, New York, NY 10021, USA

<sup>3</sup>Immunology and Microbial Pathogenesis, Weill Cornell Medical College, New York, NY 10065, USA

<sup>4</sup>Human Oncology and Pathogenesis Program, Sloan Kettering Institute, Memorial Sloan Kettering Cancer Center, New York, NY 10065, USA

<sup>5</sup>Donald B. and Catherine C. Marron Cancer Metabolism Center, Memorial Sloan Kettering Cancer Center, New York, NY 10065, USA

<sup>6</sup>Weill Cornell Medical College, New York, NY 10065, USA

<sup>7</sup>Infectious Disease Service, Department of Medicine, Memorial Sloan Kettering Cancer Center, New York, NY 10065, USA

<sup>8</sup>Lucille Castori Center for Microbes, Inflammation, and Cancer, Department of Medicine, Memorial Sloan Kettering Cancer Center, New York, NY 10065, USA

<sup>9</sup>Adult Bone Marrow Transplantation Service, Department of Medicine, Memorial Sloan Kettering Cancer Center, New York, NY 10065, USA

<sup>10</sup>Departments of Genomic Medicine and Stem Cell Transplantation Cellular Therapy, Division of Cancer Medicine, University of Texas, MD Anderson Cancer Center, Houston, TX 77030, USA

<sup>11</sup>Lead Contact

\*Correspondence: [vandenbm@mskcc.org](mailto:vandenbm@mskcc.org)

<https://doi.org/10.1016/j.chom.2018.03.002>

## SUMMARY

Bone marrow transplantation (BMT) offers curative potential for patients with high-risk hematologic malignancies, but the post-transplantation period is characterized by profound immunodeficiency. Recent studies indicate that the intestinal microbiota not only regulates mucosal immunity, but can also contribute to systemic immunity and hematopoiesis. Using antibiotic-mediated microbiota depletion in a syngeneic BMT mouse model, here we describe a role for the intestinal flora in hematopoietic recovery after BMT. Depletion of the intestinal microbiota resulted in impaired recovery of lymphocyte and neutrophil counts, while recovery of the hematopoietic stem and progenitor compartments and the erythroid lineage were largely unaffected. Depletion of the intestinal microbiota also reduced dietary energy uptake and visceral fat stores. Caloric supplementation through sucrose in the drinking water improved post-BMT hematopoietic recovery in mice with a depleted intestinal flora. Taken together, we show that the intestinal microbiota contribute to post-BMT hematopoietic reconstitution in mice through improved dietary energy uptake.

## INTRODUCTION

Allogeneic bone marrow transplantation (BMT) is an important therapy with curative potential for patients with high-risk hematologic malignancies, but the post-transplantation period is characterized by profound immunodeficiency. Delayed immune reconstitution leaves the patient susceptible to opportunistic infections and is an important contributor to transplant-related morbidity and mortality (Maury et al., 2001; Small et al., 1999). In addition, the donor immune system can exert graft-versus-tumor activity and robust reconstitution has been associated with protection against relapse of the underlying malignancy (Goldberg et al., 2017; Ishaqi et al., 2008; Michelis et al., 2014). Impaired recovery of immune function, particularly in the lymphocyte compartment, has also been described after autologous BMT (Guillaume et al., 1998) and is associated with poor overall survival (Porriata and Markovic, 2004). Thus, understanding the mechanisms by which the immune system reconstitutes and how environmental exposures might influence this process is an important objective in improving outcomes after BMT.

The intestinal microbiota plays an important role in shaping both mucosal and systemic immunity (Belkaid and Hand, 2014). Presence of an intestinal microbiota primes myelopoiesis and reduces susceptibility to infection in mice (Balmer et al., 2014; Clarke et al., 2010; Deshmukh et al., 2014; Khosravi et al., 2014; Tada et al., 1996). Polysaccharide A derived from the intestinal commensal *B. fragilis* increases CD4 T cell counts (Mazmanian et al., 2005) and the microbiota can promote the



generation of hematopoietic stem and progenitor cells (Iwamura et al., 2017; Josefsson et al., 2017; Luo et al., 2015). In addition, depletion of the intestinal flora reduces mobilization of hematopoietic stem cells (HSCs) in an experimental model of cytokine-induced peripheral HSC mobilization (Velders et al., 2004). It is thus well established that the intestinal bacteria or signals derived from them contribute to hematopoiesis. All of these studies, however, were done under steady-state conditions, and to our knowledge the role of the intestinal microbiota during the critical expansion of the hematopoietic system that occurs following BMT has not been studied.

We have previously reported that the composition of the intestinal microbiota is associated with risk for relapse of malignancy after BMT (Peled et al., 2017) and that low diversity of the post-transplant intestinal flora is associated with increased transplant-related mortality and worse overall survival in BMT patients (Taur et al., 2014). Since both relapse and transplant-related mortality are outcomes that are inversely correlated with a robust immune reconstitution (Goldberg et al., 2017; Ishaqi et al., 2008; Kim et al., 2004; Michelis et al., 2014), we hypothesized that an intact gut microbiota promotes immune reconstitution after BMT. By performing syngeneic transplantation in antibiotic (abx)-treated mice and mice with an intact intestinal flora, we demonstrate links between the microbiota, nutrition, and post-transplant hematopoiesis.

## RESULTS

### Depletion of the Intestinal Microbiota Impairs Post-BMT Hematopoiesis

To test the role of the intestinal microbiota in immune reconstitution after BMT, we performed syngeneic BMT (B6 → B6) after lethal irradiation in specific pathogen-free (SPF) mice with an intact intestinal flora and in mice treated with two different abx regimens: ampicillin + enrofloxacin (AE) and vancomycin + amikacin (VA) administered in drinking water (Figure 1A). Ampicillin and enrofloxacin are both relatively well absorbed in the intestine (Eriksson and Bolme, 1981; Heinen, 2002), while vancomycin and amikacin both have poor oral bioavailability with negligible systemic effects (Jagannath et al., 1999; Tedesco et al., 1978). Both treatments reduced the colonic bacterial abundance 1,000-fold compared to untreated control mice (Figure 1B). After BMT, we found a dramatic reduction in peripheral white blood cell (WBC) count recovery in mice treated by either of the abx regimens, while platelet (PLT) and red blood cell (RBC) counts were less affected (Figure 1C). The reduction in total WBC count could be explained to some extent by lower counts of neutrophils and monocytes, but the most dramatic difference was a 3-fold decrease in lymphocytes. Abx-treated mice had lymphocyte counts below the normal range (Figure 1C) and 5- and 3-fold reductions in B and T cell lineages, respectively (Figure 1D). Consistent with an impaired hematopoietic recovery, AE- and VA-treated mice also had lower bone marrow cellularity 28 days after BMT compared to untreated mice (Figure 1E). Importantly, abx treatment also lowered WBC and lymphocyte counts in an allogeneic, minor-MHC-antigen disparate BMT model (129 → B6; Figure S1A). To assess the functional implication of this lymphopenia, we infected mice intravenously with *Listeria monocytogenes* 21 days after BMT following a 3-day

abx washout (Figure S1B). AE-treated mice had higher bacterial load in the spleen 3 days after infection compared with untreated controls, indicating a functional immune deficit in the mice with a depleted intestinal flora (Figure S1C).

### Depletion of the Intestinal Microbiota Sensitizes Mice to Semi-Lethal Irradiation

While survival after a lethal dose of radiation requires transplantation of unexposed donor bone marrow, hematopoietic reconstitution can also be modeled by sub-lethal irradiation and subsequent endogenous hematopoietic recovery without transplant. Depletion of the flora with the AE- or VA-abx regimen sensitized mice to a 750 cGy semi-lethal irradiation dose (Figure 1F); 60% of untreated mice survived up to 60 days after irradiation, while all AE-treated mice and 90% of VA-treated mice died around day 24 after irradiation (Figure 1G). All abx-treated mice had lower lymphocyte counts and VA-treated mice had lower neutrophil counts when compared to untreated mice 14 days after irradiation (Figure S1D). The time of death (mean 24 days, range 18–31 days) indicated hematopoietic failure (Williams et al., 2010) and moribund mice had an acellular bone marrow (cells from both hindlegs totaled  $3.3\text{--}7.3 \times 10^6$ , which is less than 10% of the normal count) but no signs of infection or sepsis (no ascites or bacteria in peripheral blood or tissues). Furthermore, necropsy of AE-treated mice that were still alive 21 days after irradiation showed centrilobular hepatocellular atrophy and fatty change (Figure S1E) consistent with hypoxia due to prolonged severe anemia (Figure S1F). Mice with a depleted flora also showed reduced hematopoietic regeneration in bone marrow vertebrae compared to untreated mice (Figure 1H), possibly explaining the reduced survival of mice with a depleted flora after semi-lethal irradiation. Thus, abx-mediated depletion of the intestinal flora impairs both hematopoietic reconstitution after syngeneic BMT and autologous recovery after semi-lethal irradiation.

### Impaired Post-transplant Hematopoiesis in Abx-Treated Mice Is Mediated by Flora Depletion

We next assessed whether the detrimental effect of abx treatment on hematopoietic reconstitution is mediated by the intestinal microbiota. The effects observed after oral administration of either absorbed (AE) or non-absorbed (VA) drugs (Figures 1A–1H) suggested a microbiota-mediated effect. To verify that the impaired hematopoiesis was due to depletion of the microbial flora rather than a direct systemic effect of the abx, we utilized a colony of mice that harbor a beta-lactam-resistant microbiota by virtue of having been maintained for years under continuous abx administration (Caballero et al., 2017). One group of mice was given a fecal microbiota transfer (FMT) of the resistant flora (Res-FMT), while control mice were given an FMT with normal flora from SPF mice (Ctrl-FMT). The mice within each group were then subjected to either AE treatment or no abx and underwent BMT (Figure 1I). As expected, Res-FMT mice had sustained abundance of fecal bacteria despite AE treatment (Figure 1J) and 16S rRNA sequencing showed a diverse flora similar to that of the Res-FMT donor mice (Figures S1G and S1H). Plasma concentrations of ampicillin and enrofloxacin were not lower in Res-FMT recipients, demonstrating that the transferred resistant flora was not degrading the abx (Figure S1I). Bone marrow cellularity, WBC counts, and frequencies of

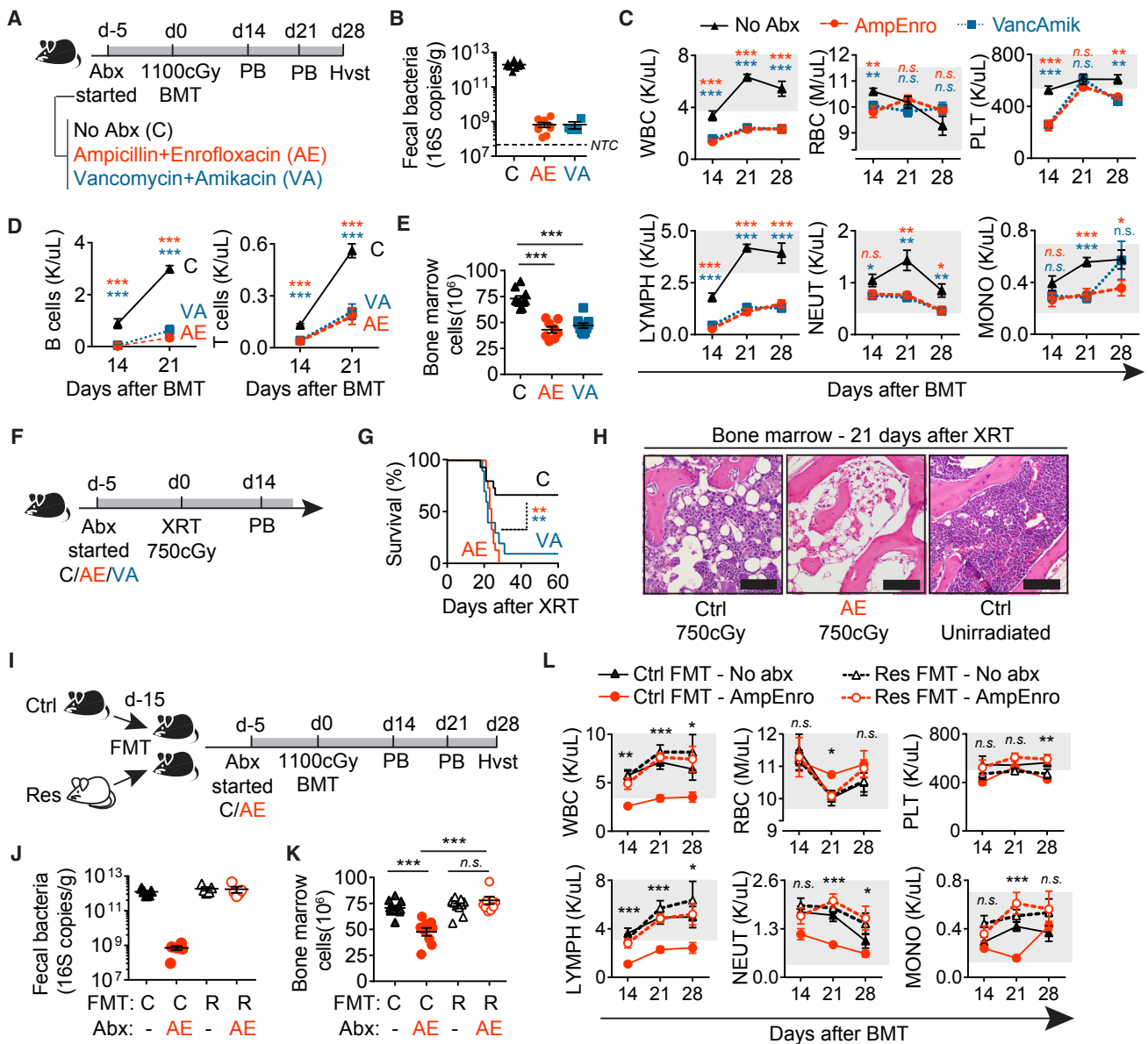


**Figure 1. Depletion of the Intestinal Microbiota Impairs Immune Reconstitution after Bone Marrow Transplantation and Sensitizes Mice to Sub-lethal Irradiation**

(A) Experimental procedure of BMT. PB, peripheral blood analysis.

(B) Quantification of bacterial 16S rRNA in fecal samples from untreated control (n = 10), ampicillin + enrofloxacin (AE)-treated (n = 10), and vancomycin + amikacin (VA)-treated mice (n = 5) 14 days after BMT. NTC, non-template control.

(C–E) White blood cells (WBC), red blood cells (RBC), platelets (PLT), lymphocytes (LYMPH), neutrophils (NEUT), and monocytes (MONO) (C); flow cytometry analysis of B and T cells in peripheral blood after BMT (D); and total bone marrow cellularity 28 days after BMT in control (n = 10), AE-treated (n = 8), and VA-treated mice (n = 10) (E).

(F) Experimental procedure of semi-lethal irradiation.

(G and H) Survival (G) and representative images (H) of hematoxylin and eosin-stained bone marrow vertebrae sections from untreated mice (left panel) and AE-treated mice (middle panel) 21 days after 750 cGy radiation and from an age-matched untreated unirradiated control mouse (right panel). Scale bar, 100  $\mu$ m.

(I) Experimental procedure of control/resistant fecal microbiota transfer (FMT) and subsequent BMT.

(J) Quantification of bacterial 16S rRNA copies in fecal samples from mice at day 0. Control (C) FMT with or without AE treatment and resistant (R) FMT with or without AE treatment (n = 5 per group).

(K and L) Total bone marrow cellularity 28 days after BMT (K) and WBC, RBC, PLT, LYMPH, NEUT, and MONO counts after BMT (L) in mice given a control FMT without (n = 10) or with (n = 9) AE treatment and mice given a resistant FMT without (n = 10) or with (n = 10) AE treatment. Significance levels are comparison of AE-treated Ctrl-FMT and AE-treated Res-FMT.

Shaded areas in (C) and (L) indicate normal ranges. \*p < 0.05, \*\*p < 0.01, \*\*\*p < 0.001; n.s., not significant. Results represent at least two independent experiments. Data are presented as mean  $\pm$  SEM. See also Figure S1.

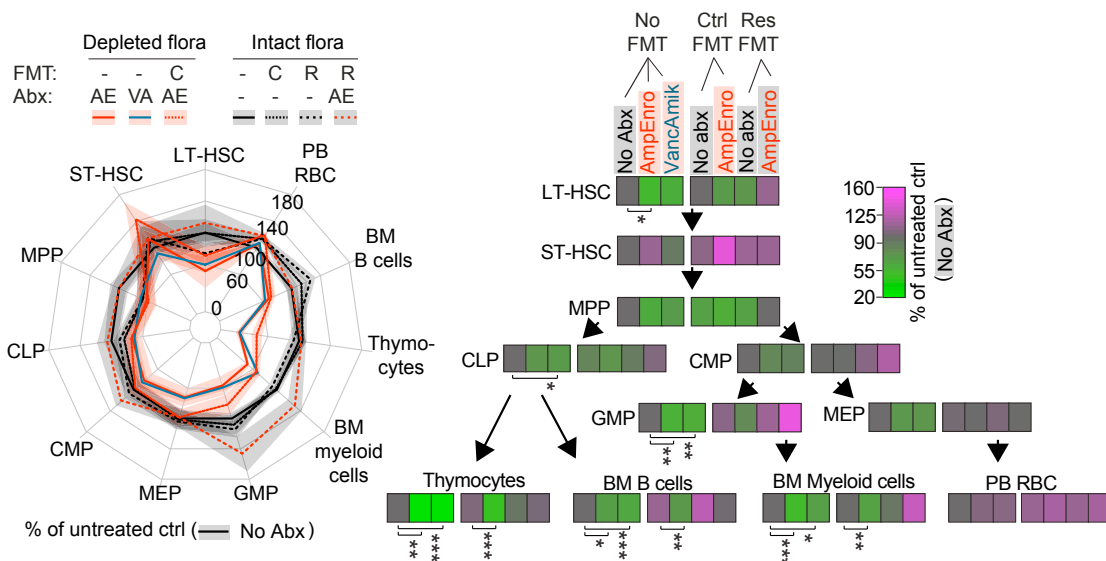


**Figure 2. Abx-Mediated Depletion of the Intestinal Microbiota Predominantly Suppresses Hematopoietic Differentiation**

Spider plot (left panel) and heatmap (right panel) of number of long-term hematopoietic stem cells (LT-HSCs, Lin<sup>-</sup>ckit<sup>+</sup>Sca1<sup>+</sup>CD150CD48<sup>-</sup>), short-term hematopoietic stem cells (ST-HSCs, Lin<sup>-</sup>ckit<sup>+</sup>Sca1<sup>+</sup>CD150<sup>-</sup>CD48<sup>-</sup>), multi-potent progenitors (MPPs, Lin<sup>-</sup>ckit<sup>+</sup>Sca1<sup>-</sup>CD48<sup>-</sup>), common lymphoid progenitors (CLPs, Lin<sup>-</sup>IL7R+ckit<sup>-</sup>), common myeloid progenitors (CMPs, Lin<sup>-</sup>ckit<sup>+</sup>Sca1<sup>-</sup>FcγR<sup>low/-</sup>CD34<sup>+</sup>), megakaryocyte-erythroid progenitors (MEPs, Lin<sup>-</sup>ckit<sup>-</sup>Sca1<sup>-</sup>FcγR<sup>-</sup>CD34<sup>+</sup>), granulocyte-monocyte progenitors (GMPs, Lin<sup>-</sup>ckit<sup>+</sup>Sca1<sup>-</sup>FcγR<sup>+</sup>CD34<sup>+</sup>), bone marrow (BM) myeloid cells (CD11b<sup>+</sup>), total thymocytes, BM B cells (B220<sup>+</sup>), and peripheral blood red blood cells (RBCs) 28 days after BMT in untreated (n = 10), AE-treated (n = 8), VA-treated (n = 10), and Ctrl-FMT mice without (n = 10) or with (n = 10) AE treatment.

Presented as percentage in relation to untreated ctrl mice (no FMT, no Abx). Results represent two independent experiments. \*p < 0.05, \*\*p < 0.01, \*\*\*p < 0.001. Data are presented as mean ± SEM. See also Figures S2 and S3.

lymphocytes and myeloid cells were effectively rescued in the AE-treated Res-FMT mice compared to AE-treated Ctrl-FMT mice (Figures 1K and 1L), demonstrating that the impaired post-BMT hematopoiesis was due to depletion of the intestinal flora and not direct effects of the abx on hematopoiesis.

### Depletion of the Intestinal Flora Impairs Lymphoid and Myeloid Differentiation

To further determine the effects of flora depletion on post-transplant hematopoiesis, we analyzed the hematopoietic stem and progenitor cell compartment 28 days after BMT. Despite an almost 50% decrease in total bone marrow cells, the number of long- and short-term hematopoietic stem cells (LT-HSCs and ST-HSCs) and multi-potent, common lymphoid, and common myeloid progenitors (MPPs, CLPs, and CMPs) was not consistently reduced in the mice with a depleted flora (AE-treated, VA-treated, or Ctrl-FMT mice treated with AE) when compared to mice with an intact intestinal flora (all untreated groups and AE-treated Res-FMT mice) (Figures 2 and S2). The reduced total bone marrow cellularity could be explained by reduced numbers of both myeloid and B lymphoid cells, while reductions in T cells were observed as lower number of thymocytes (Figures 2 and S2). Closer evaluation of differentiating B cells in the bone marrow and spleen revealed lower numbers of all cell subsets, except transitional B cells in the spleen, as well as lower total splenic cellularity in the mice with a depleted flora compared to mice with intact flora (Figures S3A–S3D). Similarly, all T cell subsets in the thymus were reduced in abx-treated mice compared to untreated mice (Fig-

ures S3E and S3F). Thus, the effects of flora depletion on post-transplant hematopoiesis present mainly as changes in expansion and differentiation of more mature cells.

Morphologic assessment of bone marrow smears revealed that the ratio of myeloid to erythroid cells was decreased in AE- and VA-treated mice compared to untreated BMT recipients (Figure S3G). Similarly, reductions were observed in the granulocyte-monocyte progenitor (GMP) compartment in AE- and VA-treated mice compared to untreated mice while numbers of megakaryocyte-erythroid progenitors (MEPs), and as previously mentioned, RBC counts were not significantly perturbed in the mice with a depleted flora (Figures 2 and S2D). In addition, *in vitro* colony-forming cultures showed equal frequencies of myeloid colony-forming units that, together with the reduced total bone marrow cellularity in mice with a depleted flora, indicated reduced numbers of GMPs (Figure S3H).

These results show that flora depletion impaired myeloid and lymphoid differentiation while largely sparing the stem and progenitor cell compartments and erythroid lineage (Figure 2). Thus, the flora is likely to influence expansion and differentiation steps in hematopoiesis.

To assess an alternative hypothesis that initial homing of donor cells to the marrow was impaired by flora depletion, we analyzed bone marrow and spleen compositions 16 hr after injection of cells. Transfer of CFSE-labeled whole-bone-marrow cells or of GFP<sup>+</sup> Lineage<sup>-</sup>Sca-1<sup>+</sup> ckit<sup>+</sup> (LSK) cells showed comparable homing in untreated mice and mice treated for 5 days with AE (Figures S3I and S3J), indicating that the gut flora did not contribute to initial homing.

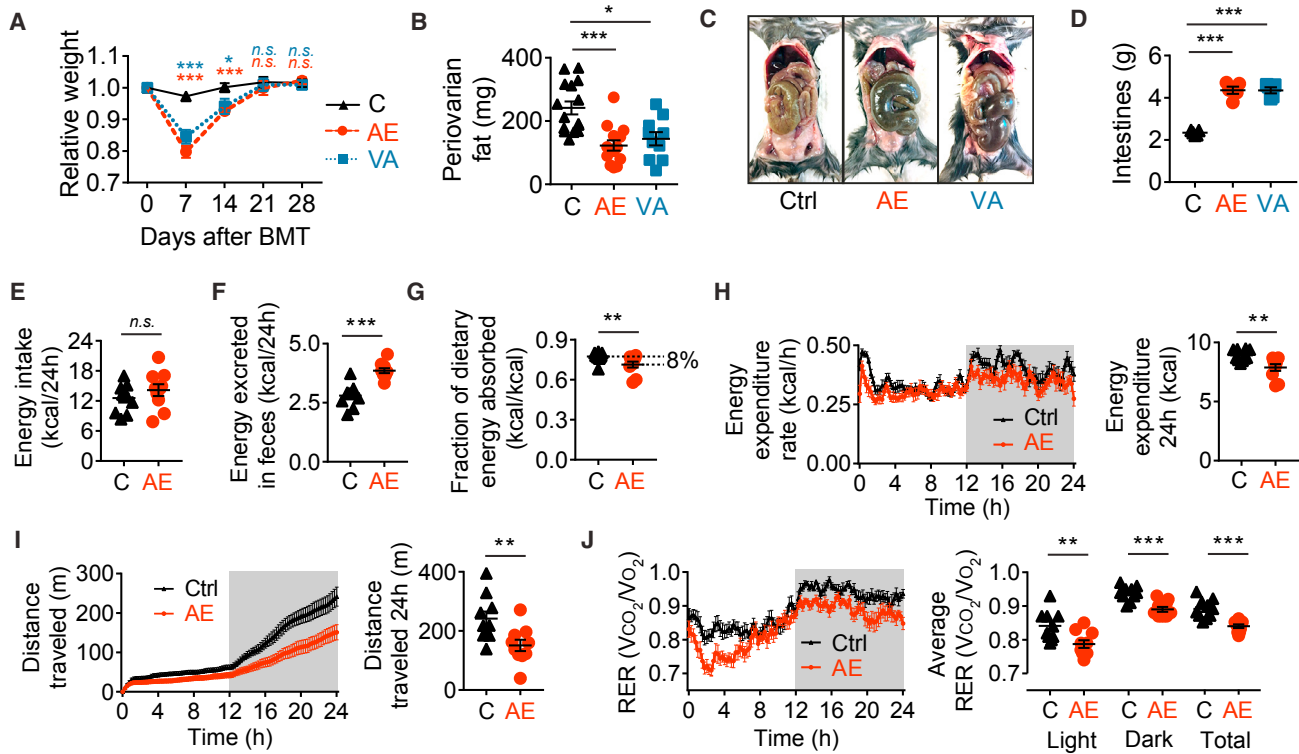


**Figure 3. Abx-Mediated Depletion of the Intestinal Microbiota Reduces Body Fat and Caloric Uptake from the Diet**

(A) Weight of untreated (n = 10), AE-treated (n = 8), and VA-treated (n = 10) mice after BMT, relative to day 0.  
(B) Weight of periovarian fat in untreated (n = 15), AE-treated (n = 14), and VA-treated (n = 10) mice 28 days after BMT.  
(C) Representative photographs of intestines and cecum in untreated, AE-treated, and VA-treated mice 28 days after BMT.  
(D) Quantification of weight of intestines and cecum including contents (from duodenum to rectum) of untreated (n = 5), AE-treated (n = 5), and VA-treated (n = 5) mice 28 days after BMT.  
(E–J) Energy intake during 24 hr (E), energy excreted as feces during 24 hr (F), fraction of energy intake absorbed (absorbed energy [ingested calories after subtraction of excreted calories] divided by ingested calories) (G), energy expenditure rate and total energy expenditure during 24 hr (H), cumulative and total distance traveled (I), and respiratory exchange ratio (RER) for untreated (n = 10) and AE-treated (n = 10) mice 13 days after BMT (J). Light and dark cycle indicated by white and gray background, respectively.

Results except (C) and (D) represent at least two independent experiments. \*p < 0.05, \*\*p < 0.01, \*\*\*p < 0.001; n.s., not significant. Data are presented as mean ± SEM. See also Figure S4.

#### Abx-Mediated Depletion of the Intestinal Flora Decreases Energy Harvest from the Diet and Reduces Visceral Adipose Tissue

In addition to showing impaired hematopoietic recovery, we noticed that the mice treated with abx lost around 20% of their body weight during the first weeks after transplant while untreated mice lost only about 3% (Figure 3A). Although all treatment groups regained their baseline weight at the end of the 28-day experiment, abx-treated mice had less visceral adipose tissue (VAT) compared to untreated mice as assessed by the amount of periovarian fat (Figure 3B), which is one of the largest VAT depots in female mice (Chusyd et al., 2016). Furthermore, the reduced weight of periovarian fat in AE-treated mice was abolished in mice harboring the abx-resistant flora (Figure S4A), indicating that the reduction in VAT deposits was mediated by depletion of the flora. As previously observed in abx-treated (Savage and Dubos, 1968) and germ-free (GF) mice (Schaefer et al., 1965), the weights of the cecum and intestines (small and large bowel) in abx-treated mice were nearly double that of untreated mice (Figures 3C and 3D). The increase in cecal

and intestinal weight accounted for about 10% of the total body weight and likely contributed to the weight re-gain of abx-treated mice, despite the loss of VAT. The cecal content also showed a darkened color in abx-treated mice compared to untreated mice, which was not the result of hematochezia as tests for occult hemoglobin in cecum and large intestine were negative (data not shown). It is known that VAT is preferentially lost when dietary restriction is implemented (Shi et al., 2007), and since the intestinal flora supports the host by breaking down complex dietary fibers that are otherwise not digestible (Bergman, 1990), we hypothesized that depletion of the flora decreased the amount of energy harvested from carbohydrates in the diet. In support of this, AE-treated mice had higher fecal output (Figure S4B) despite consuming a comparable mass of food (Figure S4C) compared to mice with an intact flora. To further determine the metabolic phenotype, AE-treated and untreated mice were singly housed in metabolic cages. The fraction of energy absorbed from the diet was 8% lower in AE-treated mice based on energy intake and energy excreted in feces (Figures 3E–3G). Abx-treated mice also had a lower energy

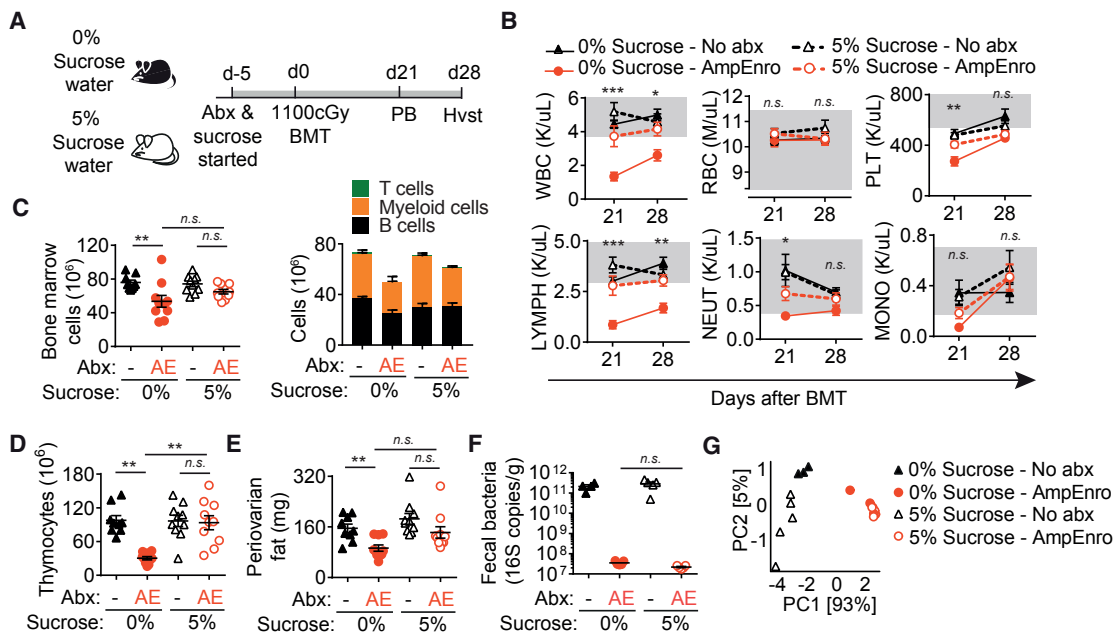


**Figure 4. Sucrose Supplementation Rescues Impaired Hematopoietic Recovery after BMT in Mice with a Depleted Flora**

(A) Experimental outline of sucrose supplementation in water and BMT. (B–E) WBC, RBC, PLT, LYMPH, NEUT, and MONO counts after BMT (B), total bone marrow cellularity and composition (C), total thymocyte count (D), and weight of periovarian fat 28 days after BMT (E) in untreated and AE-treated mice with and without 5% sucrose in drinking water ( $n = 10$  per group). (F and G) Quantification of bacterial 16S rRNA (F) and principal components 1 and 2 based on weighted normalized UniFrac analysis of 16S operational taxonomic unit (OTU) abundance (G) in fecal samples 28 days after BMT from untreated and AE-treated mice with and without administration of 5% sucrose in drinking water (untreated mice without sucrose administration,  $n = 3$ ; all other groups,  $n = 5$ ). Numbers within brackets are percent variation explained by the component. Shaded areas in (B) indicate normal ranges. Results except (F) and (G) represent two independent experiments. \* $p < 0.05$ , \*\* $p < 0.01$ , \*\*\* $p < 0.001$ ; n.s., not significant. Data are presented as mean  $\pm$  SEM. See also Figure S4.

expenditure compared to untreated mice (Figures 3H and S4D), which was partly due to less movement (Figure 3I). Reduced nutritional absorption could be a result of disrupted epithelial function in the intestine. However, intestinal epithelial integrity, as measured by leakage of FITC-dextran into the systemic circulation, was not altered in AE-treated mice compared to untreated mice (Figure S4E). Furthermore, pathology scores for intestinal apoptosis, inflammation, and erosion were not increased in AE-treated mice compared to untreated mice (Figure S4F). Metabolic profiling also showed that AE-treated transplanted mice had a higher dependence on fat metabolism compared with transplanted mice with an intact flora (Figure 3J). This was inferred from the respiratory exchange ratio (RER), which varies depending on what fuel is metabolized, with a value of 1 expected when purely carbohydrates are metabolized and a value of 0.7 expected when purely fats are metabolized (Frayn, 1983). The lower RER in AE-treated mice is thus consistent with the notion that abx-treated mice compensated for reduced caloric uptake from carbohydrates by utilizing endogenous fat, resulting in reduced VAT.

#### Sucrose Supplementation Improves Post-transplant Lymphopoiesis in Mice with an Abx-Depleted Intestinal Flora

Dietary restriction, both in experimental models and in human patients with eating disorders such as anorexia nervosa, has an impact on hematopoiesis, including reduced lymphocyte

numbers (Elegido et al., 2017; Tang et al., 2016). To test if reduced uptake of calories in flora-depleted animals contributed to impaired post-BMT hematopoiesis, we supplemented the drinking water with 5% sucrose (Figure 4A). Although not the form of energy usually provided to the host by the intestinal bacteria, sucrose is a simple carbohydrate absorbed directly by the host without the aid of the flora. This concentration has been previously shown not to induce a preference for the water and to maintain a relatively constant consumption of chow (Lewis et al., 2005), with an expected supplementation of approximately 0.9 kcal/mouse/day (about 7% of daily caloric intake). Sucrose supplementation increased peripheral WBC counts after BMT, and particularly increased the low lymphocyte count in AE-treated mice (Figure 4B). Sucrose supplementation also increased bone marrow cellularity, bone marrow B cell, and myeloid frequency, although this did not reach statistical significance (Figure 4C). In addition, sucrose-supplemented AE-treated mice had normalized thymocyte counts and showed a trend of increased periovarian VAT mass compared to non-supplemented AE-treated mice (Figures 4D and 4E). Sucrose supplementation did not alter fecal bacterial abundance or significantly shift the composition of the remaining intestinal flora in AE-treated mice (Figures 4F, 4G, and S4G). Taken together, these data suggest that sucrose supplementation can compensate for decreased post-transplant lymphopoiesis due to loss of intestinal flora.

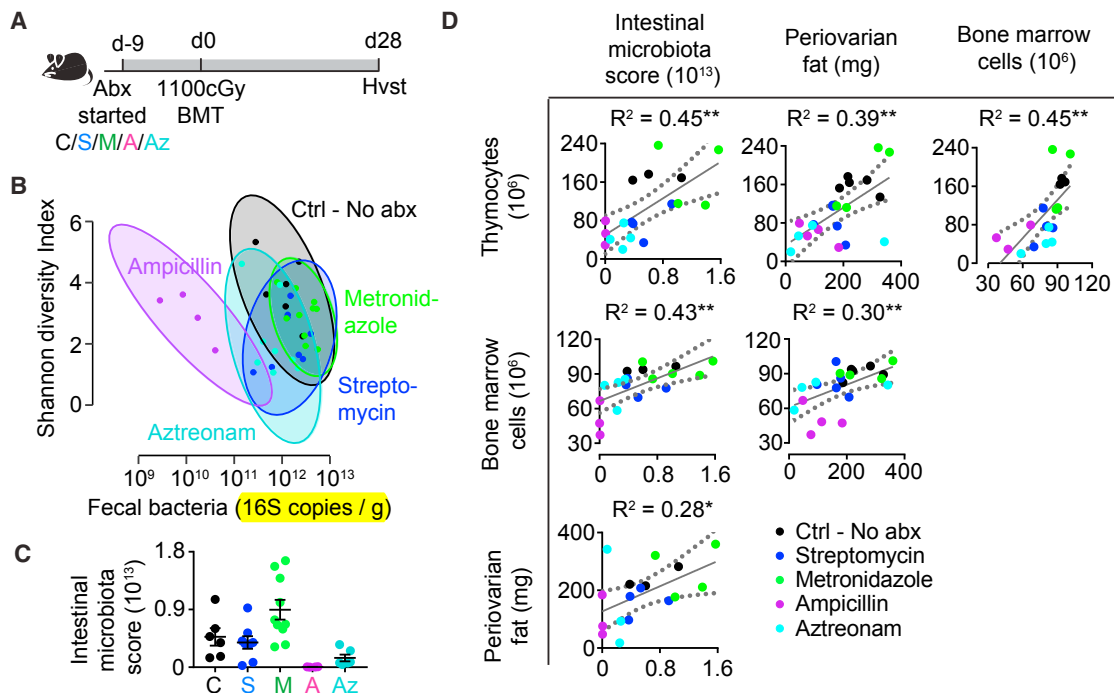


**Figure 5. Dose-Dependent Relationship between Intestinal Flora Injury and Post-BMT Hematopoiesis**

(A) Schematic outline of abx treatment and BMT.

(B) Fecal bacterial diversity (Shannon index) and fecal bacterial abundance (16S rRNA copies) in samples collected on day 0 and day 14 after BMT from untreated mice (no abx, n = 6), and mice treated with streptomycin (n = 8), metronidazole (n = 10), aztreonam (n = 6), or ampicillin (n = 4). Ellipses show 95% confidence intervals.

(C) Intestinal integrity described as an intestinal microbiota score = Shannon index  $\times$  fecal bacterial abundance for samples shown in (B).

(D) Pearson correlation of intestinal microbiota score 14 days after BMT, weight of periovarian fat, bone marrow, and thymus cellularity in untreated mice (no abx, n = 3) and mice treated with streptomycin (n = 4), metronidazole (n = 5), aztreonam (n = 4), and ampicillin (n = 3).

Results represent one experiment. \*p < 0.05, \*\*p < 0.01. Data are presented as mean  $\pm$  SEM. See also Figure S5.

### The Connection between Intestinal Flora Disruption, Reduction in Body Fat, and Impaired Post-transplant Hematopoiesis Is Dose Dependent

Having demonstrated that two different flora-depleting abx regimens impair post-transplant hematopoiesis (Figures 1 and 2), at least partly by reducing caloric uptake from the diet (Figures 3 and 4), we asked whether perturbations less severe than near-decontamination would also affect hematopoietic recovery. To generate varying degrees of microbiota perturbation, we treated mice with four abx drugs with different spectra of activity: metronidazole, streptomycin, ampicillin, and aztreonam (Figure 5A). These drugs induced variegated injury to the microbiota as assessed by their effect on total bacterial abundance (16S rRNA qPCR) and diversity (Shannon index) (Figures 5B and S5A). Despite its anaerobic-targeted spectrum, metronidazole did not induce major changes to the bacterial diversity or load except for an increase in *Faecalibaculum* (Figure S5A). Streptomycin- and aztreonam-treated mice showed a trend of reduced bacterial diversity but had bacterial loads similar to those of untreated mice, while ampicillin reduced the bacterial load dramatically (Figure 5B). In agreement with a previous study (Berg, 1981), ampicillin had the most severe effects on the intestinal flora and suppressed most intestinal bacterial strains. Therefore, the Shannon diversity index of ampicillin-treated

mice was relatively similar to that of untreated mice, since this metric relies on relative bacterial abundance and is insensitive to absolute bacterial load (Figure 5B). To obtain a parameter that summarized the degree of microbiota injury based on loss of diversity and reduction in total bacterial abundance, each fecal sample was assigned a score derived from both the bacterial diversity and load (intestinal microbiota score = Shannon Index  $\times$  16S rRNA copies per g feces) (Figure 5C). The degree of intestinal flora integrity 14 days after BMT as assessed by this score correlated positively with both amount of periovarian VAT and post-transplant hematopoietic cell levels including bone marrow cellularity and number of thymocytes 28 days after BMT (Figure 5D), further supporting the connection between the intestinal flora, nutrition, and post-transplant hematopoiesis. Total bacterial abundance as an individual value also correlated positively with immune reconstitution parameters while bacterial diversity alone did not (Figure S5B).

Ampicillin and aztreonam treatment caused comparable reductions in periovarian VAT and post-transplant lymphopoiesis as measured by thymic cellularity (Figures 5D and S5C). Interestingly, despite having similar effects on the host animal, the intestinal microbiota phenotype induced by ampicillin was a near-to-total gut decontamination, while aztreonam induced only a modest reduction in total bacterial abundance with a domination of

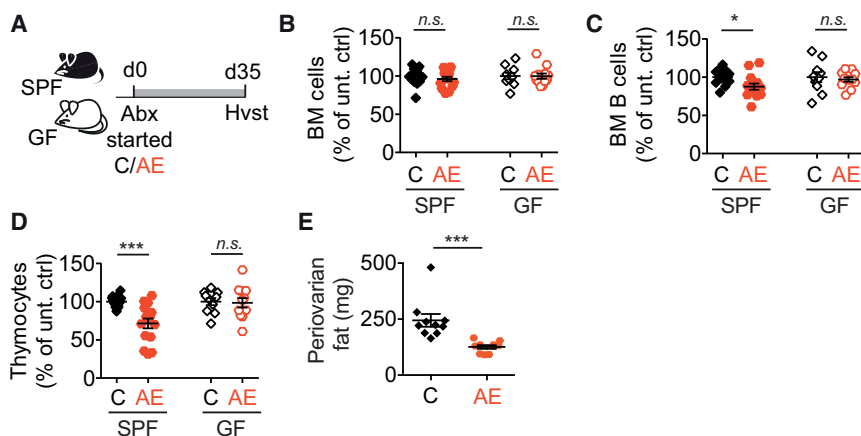


**Figure 6. Intestinal Flora Depletion Affects Steady-State Hematopoiesis**

(A) Outline of abx-treatment of mice at steady state without BMT.

(B–D) Bone marrow cellularity (B), number of bone marrow B cells ( $B220^+$ ) (C), and number of thymocytes (D) in untreated specific pathogen-free (SPF) mice ( $n = 14$ ), AE-treated SPF mice ( $n = 15$ ), untreated germ-free (GF) mice ( $n = 10$ ), and AE-treated GF mice ( $n = 12$ ) after 35 days of abx treatment.

(E) Weight of periovarian fat in untreated SPF mice ( $n = 10$ ) and AE-treated SPF mice ( $n = 10$ ) after 35 days of abx treatment.

Results represent at least two independent experiments. \* $p < 0.05$ , \*\* $p < 0.001$ ; n.s., not significant. Data are presented as mean  $\pm$  SEM. See also Figure S6.

*Blautia* (Figure S5A). Interestingly, the genomes of *Blautia* species encode relatively few enzymes active against the main dietary polysaccharides derived from plant cells (El Kaoutari et al., 2013) (Figure S5D). In contrast, genera whose genomic repertoires encode many carbohydrate-active enzymes (CAZymes), e.g., *Clostridium* and *Muribaculum*, were dramatically depleted after aztreonam treatment (Figure S5E).

Together these results suggest that the disruption of intestinal flora can influence immune reconstitution not only in a binary fashion (severe injury versus healthy), but also in a dose-dependent fashion based on both the degree of flora injury and the specific spectrum of the bacterial species affected.

#### Abx-Mediated Depletion of the Intestinal Microbiota under Steady-State Conditions Reduces Lymphocyte Numbers

Since abx-mediated flora depletion had a strong effect on the hematopoietic phenotype after BMT, we also administered the same AE regimen to non-transplanted mice to determine effects of depletion of the flora on steady-state hematopoiesis. To discriminate between effects of the abx drugs and microbiota-dependent effects, we treated both SPF and GF mice (Figure 6A). AE treatment for 5 weeks did not alter the total bone marrow cellularity in either SPF or GF mice (Figures 6B and S6A), but reduced the numbers of bone marrow B cells and thymocytes in SPF mice compared to untreated mice (Figures 6C, 6D, S6B, and S6C). These effects were not seen in the AE-treated GF mice, indicating that it was caused by depletion of the flora. Similar to the transplanted mice, the SPF steady-state AE-treated mice had reduced periovarian VAT after 5 weeks of treatment compared to untreated mice (Figure 6E), indicating that the phenomenon of abx-induced reduction in body fat was not exclusive to the post-transplant setting. Furthermore, analysis of food intake and fecal output showed comparable food intake and higher fecal output in AE-treated mice compared to untreated controls (Figures S6D and S6E), similar to the results obtained for the transplanted mice (Figures S4B and S4C).

#### DISCUSSION

In this study, we sought to determine the role of the intestinal flora on hematopoietic recovery after syngeneic BMT using an

abx-treatment mouse model. Our results show that depletion of the intestinal flora led to a profound reduction in lymphocyte counts, reduced neutrophil counts, and an impaired capacity to clear systemic infection after BMT. At the same time, initial homing of stem cells, expansion of stem and progenitor compartments, and erythroid differentiation were largely unaffected by the presence of an intact intestinal flora. That intestinal bacteria prime myeloid differentiation and improve clearance of pathogens is in line with several previous reports (Balmer et al., 2014; Clarke et al., 2010; Deshmukh et al., 2014; Khosravi et al., 2014; Tada et al., 1996), and reduced lymphocyte numbers in GF or abx-treated mice have also been described (Josefsdottir et al., 2017; Mazmanian et al., 2005). Our results show no effect or only minor effects on the hematopoietic stem and progenitor compartments in mice with a depleted intestinal flora, which is in contrast to two studies regarding HSCs in GF and abx-treated mice compared to mice with an intact flora (Iwamura et al., 2017; Josefsdottir et al., 2017). The differences between these studies and ours might be explained by (1) the use of a BMT model in our study, (2) the use of GF mice (Iwamura et al., 2017) versus abx-treated mice (our study), and (3) differences in abx regimens (Josefsdottir et al., 2017). We could also show that depletion of the intestinal flora sensitized mice to a semi-lethal dose of radiation, which is in line with previously published work demonstrating that microbiota-derived compounds can protect against irradiation-induced hematopoietic injury (Ainsworth and Mitchell, 1967; Brook and Ledney, 1994; Burdelya et al., 2008; Liu et al., 2015; Smith et al., 1958).

We observed reduced caloric uptake from the diet as a consequence of abx treatment of mice. This is in line with previous observations that dietary energy absorption increases upon bacterial colonization of GF mice (Bäckhed et al., 2004). A recent study also reported that intestinal bacteria stimulate adsorption of dietary lipids (Wang et al., 2017). Caloric restriction results in lymphopenia in both mice and humans (Elegido et al., 2017; Tang et al., 2016), and we were able to correct impaired post-BMT lymphopoiesis by supplementation of sucrose in the drinking water. Supplementation with this simple sugar rescued peripheral, thymic, and bone marrow lymphocyte counts post-BMT in abx-treated mice. The reduced numbers of neutrophils and bone marrow myeloid cells were only partly rescued by sucrose supplementation, indicating

that other mechanisms besides reduced energy extraction induced by flora depletion were involved as well. These might involve the presence of microbial-associated molecular patterns (MAMPs), which have been reported to be necessary for the maintenance of bone marrow-derived myeloid cells (Khosravi et al., 2014) or gut microbiota-derived peptidoglycans that can modulate neutrophil function (Clarke et al., 2010). The intestinal flora may contribute to energy utilization by metabolizing complex carbohydrates into simple sugars that the host can directly utilize (Bergman, 1990) and/or by modulating absorptive and functional properties of the intestines such as gut-transit time (Wichmann et al., 2013). Although we observed only a relatively minor reduction in energy extraction efficiency of about 8%, when compounded over the 28-day treatment period it is likely that this contributes to the loss of VAT after abx treatment as shown by others (Suárez-Zamorano et al., 2015). Harvest of nutrients from the diet is a well-recognized feature of the symbiotic relationship between microbiota and host across evolution (Bäckhed et al., 2005; Wong et al., 2014), and here we extend the relevance of this relationship to systemic immune recovery.

Patients undergoing allogeneic BMT have prolonged and profound nutritional alterations owing to the gastrointestinal and oral mucosal toxicities of pre-transplant conditioning regimens (Baumgartner et al., 2017; Kyle et al., 2005; Lemal et al., 2015; Papadopoulou et al., 1996), and impaired nutritional status after BMT is a negative prognostic marker of overall survival after BMT (Schulte et al., 1998). We conclude that apart from specific and direct effects of the microbiota on immuno-hematopoiesis as previously described (Balmer et al., 2014; Clarke et al., 2010; Khosravi et al., 2014; Mazmanian et al., 2005), our study demonstrates that energy harvest from the diet is a critical mechanism by which the intestinal flora contributes to hematopoiesis after BMT. This observation may help inform the development of strategies to improve immune reconstitution after transplantation.

## STAR METHODS

Detailed methods are provided in the online version of this paper and include the following:

- KEY RESOURCES TABLE
- CONTACT FOR REAGENT AND RESOURCE SHARING
- EXPERIMENTAL MODEL AND SUBJECT DETAILS
  - Mice
  - Microbial Strains
- METHOD DETAILS
  - Radiation and Bone Marrow Transplantation
  - Drug Treatments and Sucrose Supplementation
  - Listeria Infection
  - Fecal Microbiota Transfer (FMT)
  - 16S Sequencing and Quantitative PCR (qPCR)
  - Flow Cytometry
  - Colony Forming Assay and Bone Marrow Histology
  - FITC-dextran
  - Metabolic Analyses
- QUANTIFICATION AND STATISTICAL ANALYSIS
- DATA AND SOFTWARE AVAILABILITY

## SUPPLEMENTAL INFORMATION

Supplemental Information includes six figures and can be found with this article online at <https://doi.org/10.1016/j.chom.2018.03.002>.

## ACKNOWLEDGMENTS

We thank Dr. Julie R. White and coworkers at the MSKCC Center for Comparative Medicine and Pathology for pathology evaluations and Dr. Antonio Gomes for excellent computational work. This work was supported by the NIH, National Cancer Institute award number P01-CA023766 (M.R.M.v.d.B.) and Project 4 of P01-CA023766 (M.R.M.v.d.B.); NIH, National Heart, Lung, and Blood Institute award numbers R01-HL069929 (M.R.M.v.d.B.) and R01 HL124112 (R.R.J.); NIH, National Institute of Allergy and Infectious Diseases award number R01-AI100288 (M.R.M.v.d.B.); and NIH, National Institute of Diabetes and Digestive and Kidney Diseases award numbers DK048873, DK056626, and DK103046 (D.E.C.). Support was also received from The Lymphoma Foundation, The Susan and Peter Solomon Divisional Genomics Program, P30 CA008748 Memorial Sloan Kettering Cancer Center Support Grant/Core Grant, the Parker Institute for Cancer Immunotherapy at Memorial Sloan Kettering Cancer Center, the Cancer Prevention and Research Institute of Texas grant RR160089 (R.R.J.), Seres Therapeutics (J.U.P., R.R.J., and M.R.M.v.d.B.), the Swedish Research Council 2016-00149 (A.S.), the Swedish Society for Medical Research P14-0090 (A.S.), and the Swedish Society of Medicine SLS-499181 (A.S.).

## AUTHOR CONTRIBUTIONS

Conceptualization, A.S., J.U.P., R.R.J., and M.R.M.v.d.B.; Investigation A.S., M.B.d.S., A.E.S., C.S.-T., A.L., C.J.B., C.D.H., M.D.D., J.R.C., A.J.P., Y.S., B.D., E.V., J.J.T., L.J., H.J., S.L., and O.M.S.; Resources, E.G.P., D.E.C., and M.R.M.v.d.B.; Writing – Original Draft, A.S.; Writing – Review & Editing, J.U.P., R.R.J., and M.R.M.v.d.B.; Supervision, R.R.J. and M.R.M.v.d.B.

## DECLARATION OF INTERESTS

M.R.M.v.d.B. and R.R.J. are members of the scientific advisory board at Seres Therapeutics.

Received: September 12, 2017

Revised: January 30, 2018

Accepted: February 23, 2018

Published: March 22, 2018

## REFERENCES

- Ainsworth, E.J., and Mitchell, F.A. (1967). Postirradiation leukocyte patterns in mice and dogs treated with endotoxin. USNRDL-TR-67-23. Res. Dev. Tech. Rep. 1–20.
- Bäckhed, F., Ding, H., Wang, T., Hooper, L.V., Koh, G.Y., Nagy, A., Semenkovich, C.F., and Gordon, J.I. (2004). The gut microbiota as an environmental factor that regulates fat storage. Proc. Natl. Acad. Sci. USA 101, 15718–15723.
- Bäckhed, F., Ley, R.E., Sonnenburg, J.L., Peterson, D.A., and Gordon, J.I. (2005). Host-bacterial mutualism in the human intestine. Science 307, 1915–1920.
- Balmer, M.L., Schürch, C.M., Saito, Y., Geuking, M.B., Li, H., Cuenca, M., Kovtonyuk, L.V., McCoy, K.D., Hapfelmeier, S., Ochsenebein, A.F., et al. (2014). Microbiota-derived compounds drive steady-state granulopoiesis via MyD88/TICAM signaling. J. Immunol. 193, 5273–5283.
- Baumgartner, A., Bargetzi, A., Zueger, N., Bargetzi, M., Medinger, M., Bounoure, L., Gomes, F., Stanga, Z., Mueller, B., and Schuetz, P. (2017). Revisiting nutritional support for allogeneic hematologic stem cell transplantation—a systematic review. Bone Marrow Transplant. 52, 506–513.
- Belkaid, Y., and Hand, T.W. (2014). Role of the microbiota in immunity and inflammation. Cell 157, 121–141.

- Berg, R.D. (1981). Promotion of the translocation of enteric bacteria from the gastrointestinal tracts of mice by oral treatment with penicillin, clindamycin, or metronidazole. *Infect. Immun.* 33, 854–861.
- Bergman, E.N. (1990). Energy contributions of volatile fatty acids from the gastrointestinal tract in various species. *Physiol. Rev.* 70, 567–590.
- Brook, I., and Ledney, G.D. (1994). Effect of antimicrobial therapy on the gastrointestinal bacterial flora, infection and mortality in mice exposed to different doses of irradiation. *J. Antimicrob. Chemother.* 33, 63–72.
- Burdelya, L.G., Krivokrysenko, V.I., Tallant, T.C., Strom, E., Gleiberman, A.S., Gupta, D., Kurnasov, O.V., Fort, F.L., Osterman, A.L., Didonato, J.A., et al. (2008). An agonist of toll-like receptor 5 has radioprotective activity in mouse and primate models. *Science* 320, 226–230.
- Caballero, S., Kim, S., Carter, R.A., Leiner, I.M., Sušac, B., Miller, L., Kim, G.J., Ling, L., and Pamer, E.G. (2017). Cooperating commensals restore colonization resistance to vancomycin-resistant *Enterococcus faecium*. *Cell Host Microbe* 21, 592–602.e4.
- Charles River. (2012). C57BL/6 mouse hematology North American Colonies. <https://www.criver.com/>.
- Chusyd, D.E., Wang, D., Huffman, D.M., and Nagy, T.R. (2016). Relationships between rodent white adipose fat pads and human white adipose fat depots. *Front Nutr* 3, 10.
- Clarke, T.B., Davis, K.M., Lysenko, E.S., Zhou, A.Y., Yu, Y., and Weiser, J.N. (2010). Recognition of peptidoglycan from the microbiota by Nod1 enhances systemic innate immunity. *Nat. Med.* 16, 228–231.
- Clifford, R.J., Milillo, M., Prestwood, J., Quintero, R., Zurawski, D.V., Kwak, Y.I., Waterman, P.E., Lesho, E.P., and Mc Gann, P. (2012). Detection of bacterial 16S rRNA and identification of four clinically important bacteria by real-time PCR. *PLoS One* 7, e48558.
- Deshmukh, H.S., Liu, Y., Menkiti, O.R., Mei, J., Dai, N., O'Leary, C.E., Oliver, P.M., Kolls, J.K., Weiser, J.N., and Worthen, G.S. (2014). The microbiota regulates neutrophil homeostasis and host resistance to *Escherichia coli* K1 sepsis in neonatal mice. *Nat. Med.* 20, 524–530.
- El Kaoutari, A., Armougom, F., Gordon, J.I., Raoult, D., and Henrissat, B. (2013). The abundance and variety of carbohydrate-active enzymes in the human gut microbiota. *Nat. Rev. Microbiol.* 11, 497–504.
- Elegido, A., Graell, M., Andrés, P., Gheorghe, A., Marcos, A., and Nova, E. (2017). Increased naive CD4<sup>+</sup> and B lymphocyte subsets are associated with body mass loss and drive relative lymphocytosis in anorexia nervosa patients. *Nutr. Res.* 39, 43–50.
- Eriksson, M., and Bolme, P. (1981). The oral absorption of ampicillin, pivampicillin and amoxycillin in infants and children. *Acta Pharmacol. Toxicol. (Copenh.)* 49, 38–42.
- Frayn, K.N. (1983). Calculation of substrate oxidation rates in vivo from gaseous exchange. *J. Appl. Physiol.* 55, 628–634.
- Goldberg, J.D., Zheng, J., Ratan, R., Small, T.N., Lai, K.C., Boulad, F., Castro-Malaspina, H., Giralt, S.A., Jakubowski, A.A., Kernan, N.A., et al. (2017). Early recovery of T-cell function predicts improved survival after T-cell depleted allogeneic transplant. *Leuk. Lymphoma* 58, 1859–1871.
- Guillaume, T., Rubinstein, D.B., and Symann, M. (1998). Immune reconstitution and immunotherapy after autologous hematopoietic stem cell transplantation. *Blood* 92, 1471–1490.
- Heinen, E. (2002). Comparative serum pharmacokinetics of the fluoroquinolones enrofloxacin, difloxacin, marbofloxacin, and orbifloxacin in dogs after single oral administration. *J. Vet. Pharmacol. Ther.* 25, 1–5.
- Honorato, R.V. (2016). CAZy-parser a way to extract information from the Carbohydrate-Active enZYmes Database. *J. Open Source Softw.* 1, 53.
- Ishaqi, M.K., Afzal, S., Dupuis, A., Doyle, J., and Gassas, A. (2008). Early lymphocyte recovery post-allogeneic hematopoietic stem cell transplantation is associated with significant graft-versus-leukemia effect without increase in graft-versus-host disease in pediatric acute lymphoblastic leukemia. *Bone Marrow Transplant.* 41, 245–252.
- Iwamura, C., Bouladoux, N., Belkaid, Y., Sher, A., and Jankovic, D. (2017). Sensing of the microbiota by NOD1 in mesenchymal stromal cells regulates murine hematopoiesis. *Blood* 129, 171–176.
- Jagannath, C., Wells, A., Mshvildadze, M., Olsen, M., Sepulveda, E., Emanuele, M., Hunter, R.L., Jr., and Dasgupta, A. (1999). Significantly improved oral uptake of amikacin in FVB mice in the presence of CRL-1605 copolymer. *Life Sci.* 64, 1733–1738.
- Josefsdottir, K.S., Baldridge, M.T., Kadmon, C.S., and King, K.Y. (2017). Antibiotics impair murine hematopoiesis by depleting the intestinal microbiota. *Blood* 129, 729–739.
- Khosravi, A., Yáñez, A., Price, J.G., Chow, A., Merad, M., Goodridge, H.S., and Mazmanian, S.K. (2014). Gut microbiota promote hematopoiesis to control bacterial infection. *Cell Host Microbe* 15, 374–381.
- Kim, D.H., Kim, J.G., Sohn, S.K., Sung, W.J., Suh, J.S., Lee, K.S., and Lee, K.B. (2004). Clinical impact of early absolute lymphocyte count after allogeneic stem cell transplantation. *Br. J. Haematol.* 125, 217–224.
- Kyle, U.G., Chalandon, Y., Miralbell, R., Karsegard, V.L., Hans, D., Trombetti, A., Rizzoli, R., Helg, C., and Pichard, C. (2005). Longitudinal follow-up of body composition in hematopoietic stem cell transplant patients. *Bone Marrow Transplant.* 35, 1171–1177.
- Lemal, R., Cabrespine, A., Pereira, B., Combal, C., Ravinet, A., Hermet, E., Bay, J.O., and Bouteloup, C. (2015). Could enteral nutrition improve the outcome of patients with haematological malignancies undergoing allogeneic haematopoietic stem cell transplantation? A study protocol for a randomized controlled trial (the NEPHA study). *Trials* 16, 136.
- Lewis, S.R., Ahmed, S., Dym, C., Khaimova, E., Kest, B., and Bodnar, R.J. (2005). Inbred mouse strain survey of sucrose intake. *Physiol. Behav.* 85, 546–556.
- Liu, W., Chen, Q., Wu, S., Xia, X., Wu, A., Cui, F., Gu, Y.P., Zhang, X., and Cao, J. (2015). Radioprotector WR-2721 and mitigating peptidoglycan synergistically promote mouse survival through the amelioration of intestinal and bone marrow damage. *J. Radiat. Res. (Tokyo)* 56, 278–286.
- Lombard, V., Golaconda Ramulu, H., Drula, E., Coutinho, P.M., and Henrissat, B. (2014). The carbohydrate-active enzymes database (CAZy) in 2013. *Nucleic Acids Res.* 42, D490–D495.
- Lozupone, C., Hamady, M., and Knight, R. (2006). UniFrac—an online tool for comparing microbial community diversity in a phylogenetic context. *BMC Bioinformatics* 7, 371.
- Luo, Y., Chen, G.L., Hannemann, N., Ipseiz, N., Krönke, G., Bäuerle, T., Munos, L., Wirtz, S., Schett, G., and Bozec, A. (2015). Microbiota from obese mice regulate hematopoietic stem cell differentiation by altering the bone niche. *Cell Metab.* 22, 886–894.
- Maury, S., Mary, J.Y., Rabian, C., Schwarzinger, M., Toubert, A., Scieux, C., Carmagnat, M., Esperou, H., Ribaud, P., Devergie, A., et al. (2001). Prolonged immune deficiency following allogeneic stem cell transplantation: risk factors and complications in adult patients. *Br. J. Haematol.* 115, 630–641.
- Mazmanian, S.K., Liu, C.H., Tzianabos, A.O., and Kasper, D.L. (2005). An immunomodulatory molecule of symbiotic bacteria directs maturation of the host immune system. *Cell* 122, 107–118.
- Michelis, F.V., Messner, H.A., Loach, D., Uhm, J., Gupta, V., Lipton, J.H., Seftel, M.D., Kuruvilla, J., and Kim, D.D. (2014). Early lymphocyte recovery at 28 d post-transplant is predictive of reduced risk of relapse in patients with acute myeloid leukemia transplanted with peripheral blood stem cell grafts. *Eur. J. Haematol.* 93, 273–280.
- Papadopoulou, A., Lloyd, D.R., Williams, M.D., Derbyshire, P.J., and Booth, I.W. (1996). Gastrointestinal and nutritional sequelae of bone marrow transplantation. *Arch. Dis. Child.* 75, 208–213.
- Peled, J.U., Devlin, S.M., Staffas, A., Lumish, M., Khanin, R., Littmann, E.R., Ling, L., Kosuri, S., Maloy, M., Slingerland, J.B., et al. (2017). Intestinal microbiota and relapse after hematopoietic-cell transplantation. *J. Clin. Oncol.* 35, 1650–1659.
- Porrata, L.F., and Markovic, S.N. (2004). Timely reconstitution of immune competence affects clinical outcome following autologous stem cell transplantation. *Clin. Exp. Med.* 4, 78–85.
- Savage, D.C., and Dubos, R. (1968). Alterations in the mouse cecum and its flora produced by antibacterial drugs. *J. Exp. Med.* 128, 97–110.

- Schaedler, R.W., Dubs, R., and Costello, R. (1965). Association of germfree mice with bacteria isolated from normal mice. *J. Exp. Med.* 122, 77–82.
- Schloss, P.D., Westcott, S.L., Ryabin, T., Hall, J.R., Hartmann, M., Hollister, E.B., Lesniewski, R.A., Oakley, B.B., Parks, D.H., Robinson, C.J., et al. (2009). Introducing mothur: open-source, platform-independent, community-supported software for describing and comparing microbial communities. *Appl. Environ. Microbiol.* 75, 7537–7541.
- Schloss, P.D., Gevers, D., and Westcott, S.L. (2011). Reducing the effects of PCR amplification and sequencing artifacts on 16S rRNA-based studies. *PLoS One* 6, e27310.
- Schulte, C., Reinhardt, W., Beelen, D., Mann, K., and Schaefer, U. (1998). Low T3-syndrome and nutritional status as prognostic factors in patients undergoing bone marrow transplantation. *Bone Marrow Transplant.* 22, 1171–1178.
- Shi, H., Strader, A.D., Woods, S.C., and Seeley, R.J. (2007). Sexually dimorphic responses to fat loss after caloric restriction or surgical lipectomy. *Am. J. Physiol. Endocrinol. Metab.* 293, E316–E326.
- Small, T.N., Papadopoulos, E.B., Boulad, F., Black, P., Castro-Malaspina, H., Childs, B.H., Collins, N., Gillio, A., George, D., Jakubowski, A., et al. (1999). Comparison of immune reconstitution after unrelated and related T-cell-depleted bone marrow transplantation: effect of patient age and donor leukocyte infusions. *Blood* 93, 467–480.
- Smith, W.W., Alderman, I.M., and Gillespie, R.E. (1958). Hematopoietic recovery induced by bacterial endotoxin in irradiated mice. *Am. J. Physiol.* 192, 549–556.
- Suárez-Zamorano, N., Fabbiano, S., Chevalier, C., Stojanović, O., Colin, D.J., Stevanović, A., Veyrat-Durebex, C., Tarallo, V., Rigo, D., Germain, S., et al. (2015). Microbiota depletion promotes browning of white adipose tissue and reduces obesity. *Nat. Med.* 21, 1497–1501.
- Tada, T., Yamamura, S., Kuwano, Y., and Abo, T. (1996). Level of myelopoiesis in the bone marrow is influenced by intestinal flora. *Cell. Immunol.* 173, 155–161.
- Tang, D., Tao, S., Chen, Z., Koliesnik, I.O., Calmes, P.G., Hoerr, V., Han, B., Gebert, N., Zörnig, M., Löffler, B., et al. (2016). Dietary restriction improves repopulation but impairs lymphoid differentiation capacity of hematopoietic stem cells in early aging. *J. Exp. Med.* 213, 535–553.
- Taur, Y., Jenq, R.R., Perales, M.A., Littmann, E.R., Morjaria, S., Ling, L., No, D., Gobourne, A., Viale, A., Dahl, P.B., et al. (2014). The effects of intestinal tract bacterial diversity on mortality following allogeneic hematopoietic stem cell transplantation. *Blood* 124, 1174–1182.
- Tedesco, F., Markham, R., Gurwith, M., Christie, D., and Bartlett, J.G. (1978). Oral vancomycin for antibiotic-associated pseudomembranous colitis. *Lancet* 2, 226–228.
- Turnbaugh, P.J., Hamady, M., Yatsunenko, T., Cantarel, B.L., Duncan, A., Ley, R.E., Sogin, M.L., Jones, W.J., Roe, B.A., Affourtit, J.P., et al. (2009). A core gut microbiome in obese and lean twins. *Nature* 457, 480–484.
- Velders, G.A., van Os, R., Hagoort, H., Verzaal, P., Guiot, H.F., Lindley, I.J., Willemze, R., Opdenakker, G., and Fibbe, W.E. (2004). Reduced stem cell mobilization in mice receiving antibiotic modulation of the intestinal flora: involvement of endotoxins as cofactors in mobilization. *Blood* 103, 340–346.
- Wang, Y., Kuang, Z., Yu, X., Ruhn, K.A., Kubo, M., and Hooper, L.V. (2017). The intestinal microbiota regulates body composition through NFIL3 and the circadian clock. *Science* 357, 912–916.
- Weir, J.B. (1949). New methods for calculating metabolic rate with special reference to protein metabolism. *J. Physiol.* 109, 1–9.
- Wichmann, A., Allahyar, A., Greiner, T.U., Plovier, H., Lundén, G.O., Larsson, T., Drucker, D.J., Delzenne, N.M., Cani, P.D., and Bäckhed, F. (2013). Microbial modulation of energy availability in the colon regulates intestinal transit. *Cell Host Microbe* 14, 582–590.
- Williams, J.P., Brown, S.L., Georges, G.E., Hauer-Jensen, M., Hill, R.P., Huser, A.K., Kirsch, D.G., Macvittie, T.J., Mason, K.A., Medhora, M.M., et al. (2010). Animal models for medical countermeasures to radiation exposure. *Radiat. Res.* 173, 557–578.
- Wong, A.C., Dobson, A.J., and Douglas, A.E. (2014). Gut microbiota dictates the metabolic response of *Drosophila* to diet. *J. Exp. Biol.* 217, 1894–1901.

**STAR★METHODS****KEY RESOURCES TABLE**

REAGENT or RESOURCE	SOURCE	IDENTIFIER
<b>Antibodies</b>		
CD4-Brilliant Violet 711 (clone RM4-5)	BioLegend	Cat# 100549 RRID: AB_11219396
CD8-Brilliant Violet 785 (clone 53-6.7)	BioLegend	Cat# 100749 RRID: AB_11218801
B220-PE (clone RA6-6B2)	BD Biosciences	Cat# 553084 RRID: AB_394614
Gr1-APC (clone PK136)	BD Biosciences	Cat# 553129 RRID: AB_398532
Mac1-PE-Cy7 (clone M1/70)	BD Biosciences	Cat# 552850 RRID: AB_394491
CD45.1-Brilliant Violet 650 (clone A20)	BioLegend	Cat# 110735 RRID: AB_11124743
CD45.2 PerCp-Cy5.5 (clone 104)	BD Biosciences	Cat# 552950 RRID: AB_394528
Sca1-PE-Cy7 (clone D7)	BD Biosciences	Cat# 558162 RRID: AB_647253
ckit-APC (clone 2B8)	BD Biosciences	Cat# 553356 RRID: AB_398536
IL7Ra-APC-e780 (clone A7R34)	Thermo Fisher Scientific	Cat# 45-1278-73 RRID: AB_906210
CD48-FITC (clone HM48-1)	BD Biosciences	Cat# 557484 RRID: AB_396724
CD150-PerCp-eFlour 710 (clone mShad150)	Thermo Fisher Scientific	Cat# 46-1502-82 RRID: AB_2016699
CD34-Alexa-700	BD Biosciences	Cat# 560518 RRID: AB_1727471
CD16/CD32-eFlour450 (clone 93)	Thermo Fisher Scientific	Cat# 48-0161-82 RRID: AB_1272191
Gr1-biotin (clone RB6-8C5)	BD Biosciences	Cat# 553125 RRID: AB_394641
CD3-biotin (clone 145-2C11)	BD Biosciences	Cat# 553060 RRID: AB_394593
NK1.1-biotin (clone PK136)	BD Biosciences	Cat# 553163 RRID: AB_394675
CD11b-biotin (clone M1/70)	BD Biosciences	Cat# 553309 RRID: AB_394773
CD11c-biotin (clone HL3)	BD Biosciences	Cat# 553800 RRID: AB_395059
CD8-biotin (clone 53-6.7)	BD Biosciences	Cat# 553029 RRID: AB_394567
CD4-biotin (clone RM4-5)	BD Biosciences	Cat# 553044 RRID: AB_394580
Ter119-biotin (clone TER-119)	BD Biosciences	Cat# 553672 RRID: AB_394985
CD19-biotin (clone ID3)	BD Biosciences	Cat# 553784 RRID: AB_395048
CD25-PE-Cy7 (clone PC61)	Thermo Fisher Scientific	Cat# 25-0251-82 RRID: AB_469608
CD44-eFlour450 (clone IM7)	Thermo Fisher Scientific	Cat# 48-0441-82 RRID: AB_1272246
B220-Brilliant Violet 650 (clone RA3-6B2)	BioLegend	Cat# 103241 RRID: AB_11204069
CD43-FITC (clone S7)	BD Biosciences	Cat# 553270 RRID: AB_394747
IgM-PE/Cy7 (clone RMM-1)	BioLegend	Cat# 406513 RRID: AB_10640069
IgD-Alexa Fluor 700 (clone 11-26c.2a)	BioLegend	Cat# 405729 RRID: AB_2563340
Ly-51-PE (clone BP-1)	BD Biosciences	Cat# 553735 RRID: AB_395018
CD24/HSA-Biotin (clone M1/69)	BD Biosciences	Cat# 553260 RRID: AB_394739
CD19-APC (clone 1D3)	BD Biosciences	Cat# 550992 RRID: AB_398483
CD93-FITC (clone AA4.1)	Thermo Fisher Scientific	Cat# 11-5892-82 RRID: AB_465298
CD21/CD35-APC/Cy7 (clone 7Eq)	BioLegend	Cat# 123417 RRID: AB_1953274
<b>Bacterial and Virus Strains</b>		
<i>Listeria monocytogenes</i> strain 10403s	N/A	N/A
<b>Chemicals, Peptides, and Recombinant Proteins</b>		
CellTrace CFSE Cell Proliferation Kit	Thermo Fisher Scientific	Cat# C34554
Ampicillin	GoldBio	Cat# A-301-5
Enrofloxacin	Sigma-Aldrich	Cat# 17849
Vancomycin	MP Biomedicals	Cat# 219554005
Amikacin	Cayman Chemical	Cat# 15405
Metronidazole	Sigma-Aldrich	Cat# M3761
Streptomycin	Sigma-Aldrich	Cat# S9137

(Continued on next page)

**Continued**

REAGENT or RESOURCE	SOURCE	IDENTIFIER
Aztreonam	Nova Plus Pharmaceuticals	Cat# 63323040120
Sucrose	Sigma-Aldrich	Cat# 16104
Streptavidin-Qdot605	Thermo Fisher Scientific	Cat# Q10103MP
Streptavidin-BV785	BioLegend	Cat# 405249
Critical Commercial Assays		
PowerUp SyberGreen mastermix	Thermo Fisher Scientific	Thermo Fisher Scientific Cat#: A25742
BD Pharm Lyse	BD Biosciences	BD Biosciences Cat#: 555899
MethoCult GF M3434	Stem Cell Technologies	Stem Cell Technologies Cat#: M3434
Deposited Data		
16S rRNA sequencing	European Nucleotide Archive (ENA)	ENA: PRJEB24887
Experimental Models: Organisms/Strains		
Mouse: C57BL6/J	The Jackson Laboratory	JAX Cat# 000664; RRID: IMSR_JAX:000664
Mouse: 129S1/SvImJ	The Jackson Laboratory	JAX Cat# 002448; RRID: IMSR_JAX:002448
Mouse: B6.SJL-PtprcaPepc <sup>b</sup> /Boy (Ly5.1)	The Jackson Laboratory	JAX Cat# 002014; RRID: IMSR_JAX:002014
Mouse: C57BL/6-Tg(UBC-GFP)30Scha/J	The Jackson Laboratory	JAX Cat# 004353; RRID: IMSR_JAX:004353
Oligonucleotides		
16S_qPCR-F 5'-ACT CCT ACG GGA GGC AGC AGT-3'	(Clifford et al., 2012)	N/A
16S_qPCR-R 5'-TAT TAC CGC GGC TGC TGG C -3'	(Clifford et al., 2012)	N/A
Software and Algorithms		
Mothur v1.34	(Schloss et al., 2009)	<a href="https://www.mothur.org">https://www.mothur.org</a> ; RRID: SCR_011947
R v3.4.0	N/A	<a href="http://www.r-project.org">http://www.r-project.org</a> ; RRID: SCR_001905
NCBI BLASTN	N/A	<a href="https://blast.ncbi.nlm.nih.gov/">https://blast.ncbi.nlm.nih.gov/</a> ; RRID: SCR_001598
CAZy database	(Lombard et al., 2014)	<a href="http://www.cazy.org">http://www.cazy.org</a> ; RRID: SCR_012909
CAZy parser	(Honorato, 2016)	<a href="https://github.com/rodrigovrgs/cazy-parser">https://github.com/rodrigovrgs/cazy-parser</a>
GraphPad Prism v6.07	GraphPad Software	<a href="https://www.graphpad.com/">https://www.graphpad.com/</a> ; RRID: SCR_002798
FlowJo	FlowJo LLC	<a href="https://www.flowjo.com/">https://www.flowjo.com/</a> ; RRID: SCR_008520

**CONTACT FOR REAGENT AND RESOURCE SHARING**

Further information and requests for resources and reagents should be directed to and will be fulfilled by the Lead Contact, Marcel R.M. van den Brink ([vandenbm@mskcc.org](mailto:vandenbm@mskcc.org)).

**EXPERIMENTAL MODEL AND SUBJECT DETAILS****Mice**

Mice were kept under specific pathogen-free conditions except where germ-free conditions are specified and maintained on a 12 hour light/dark cycle with unlimited access to water and food (5053 Rodent Diet 20, PicoLab). Female mice were used to facilitate randomized mixing between the experimental groups prior to every experiment. C57BL6/J mice were used as host and bone marrow cells for transplantation were prepared from female B6.SJL-PtprcaPepc<sup>b</sup>/Boy (Ly5.1) or female 129S1/SvImJ mice. All mice were obtained from Jackson Laboratories and used at 8 – 10 weeks of age. All experiments were performed using protocols approved by the Memorial Sloan Kettering Cancer Center (MSKCC) Institutional animal care and use committee (IACUC).

**Microbial Strains**

*Listeria monocytogenes* 10403s was cultured in suspension in BBL brain-heart-infusion media or on BBL brain-heart-infusion agar plates for enumeration. *Listeria monocytogenes* at log-phase growth was mixed with autoclaved glycerol (20% final concentration) and kept as stocks at -80°C.

## METHOD DETAILS

### Radiation and Bone Marrow Transplantation

Mice were given a split 1100cGy radiation dose and administered  $5 \times 10^6$  bone marrow cells via tail vein injection. A single 750cGy radiation dose was used to test endogenous reconstitution. For analysis of homing,  $5 \times 10^6$  CFSE-stained bone marrow cells or  $2 \times 10^4$  Lineage<sup>-</sup>Sca1<sup>+</sup>ckit<sup>+</sup> cells sorted from the bone marrow of GFP<sup>+</sup> B6 mice (C57BL/6-Tg(UBC-GFP)30Scha/J) were injected via the tail vein and organs harvested 16h later. Complete blood counts from sub-mandibular bleeds were analyzed using a ProCyte Dx Hematology Analyzer (IDEXX Laboratories). Normal CBC ranges were based on data from the C57BL/6 North American Colonies (Charles River, 2012).

### Drug Treatments and Sucrose Supplementation

Ampicillin 0.5 g/L and enrofloxacin 0.25 g/L or vancomycin 0.5 g/L and amikacin 0.5 g/L, were given in the drinking water starting 5 days before BMT and throughout the experiment. Metronidazole 0.5 g/L, streptomycin 5 g/L, or aztreonam 0.5 g/L were started 9 days before BMT and administered throughout the experiment. Ampicillin 0.5 g/L and enrofloxacin 0.25 g/L treatment without BMT was administered in the drinking water for 35 days. Abx water was changed at least every 5–7 days. Sucrose was supplemented (50 g/L) in drinking water and changed every 2–3 days.

### Listeria Infection

Abx treatment was stopped 3 days prior to infection to allow for washout of the abx. Cultured *Listeria monocytogenes* 10403s was diluted in PBS and  $5 \times 10^3$  CFUs were administered intravenously via tail vein. Infected mice were euthanized 3 days later, spleen and liver mashed through a 100 µm cell strainer in PBS+0.05%Triton, and plated in serial dilutions on brain-heart-infusion agar plates to assess bacterial load.

### Fecal Microbiota Transfer (FMT)

Cecal content solution for FMT was prepared from untreated C57BL6/J or from Myd88KO mice under continuous amoxicillin treatment (Caballero et al., 2017). The cecum was placed in an anaerobic chamber and its contents were dissolved in 6 ml PBS. Recipient mice were given ampicillin 0.5 g/L and enrofloxacin 0.25 g/L in the drinking water for 72 h and abx were removed 24 h before FMT was administered as a single dose of 200 µl cecal content solution by oral gavage.

### 16S Sequencing and Quantitative PCR (qPCR)

DNA from fecal pellets from individual mice was purified using phenol-chloroform extraction with mechanical disruption (bead beating) based on a previously described protocol (Turnbaugh et al., 2009). Bacterial DNA was analyzed using the Illumina MiSeq platform to sequence the V4-V5 region of the 16S rRNA gene. Sequence data were compiled and processed using mothur and screened and filtered for quality (Schloss et al., 2011). Operational taxonomic units (OTUs) were classified to the genus level using NCBI blastn and the alignment hit with the highest score. Principal component analysis was performed upon a weighted and normalized UniFrac (Lozupone et al., 2006) distance matrix of OTU abundance in R software. Abundance of total 16S rRNA copies was analyzed by qPCR using SyberGreen mastermix, 16S\_qPCR-F and 16S\_qPCR-R oligonucleotides on a StepOnePlus RealTime PCR System (Applied Biosystems) with a standard curve based on serial dilutions of a *Blautia* 16S rRNA sequence cloned into the pcDNA4 plasmid.

### Flow Cytometry

Bone marrow cells, thymocytes, splenocytes, or peripheral blood cells were suspended in PBS with 2mM EDTA and 5% FCS. Red cells were lysed from bone marrow and peripheral blood cells using BD Pharm Lyse. Mature blood cells were characterized in peripheral blood or bone marrow using CD4-BV711, CD8-BV785, B220-PE, Gr1-APC, Mac1-PE-Cy7, CD45.1-BV650, and CD45.2-PerCp-Cy5.5. Bone marrow stem cells and progenitor cells were characterized using Sca1-PE-Cy7, ckit-APC, IL7Ra-APC-e780, CD48-FITC, CD150-PerCp-Cy5.5, CD34-Alexa-700, CD16/CD32-eFlour450 and a biotin-conjugated lineage cocktail containing antibodies against Gr1, CD3, NK1.1, CD11b, CD11c, CD8, CD4, Ter119, and CD19, and stained secondary with Streptavidin-Qdot605. Thymocytes were analyzed using CD4-BV711 and CD8-BV785. B cell subsets in bone marrow were characterized using B220-BV650, CD43-FITC, IgM-Pe-Cy7, IgD-Alexa700, Ly-51-PE and CD24/HSA-Biotin secondary stained with Streptavidin-BV785. B cell subsets in the spleen were analyzed using CD19-APC, CD93-FITC, IgM-Pe-Cy7, and CD21/35-APC-Cy7. DAPI was used to exclude dead cells. Stained cells were analyzed on a BD LSR II and data analyzed using FlowJo software.

### Colony Forming Assay and Bone Marrow Histology

Myeloid colony forming assays were performed by plating  $2 \times 10^4$  bone marrow cells, counted after lysis of red cells, in duplicates in methyl cellulose media supplemented with growth factors. Colonies were counted 12 days later. Morphologic bone marrow assessment was done on Wright-Giemsa-stained bone marrow brushings using an Olympus BX46 microscope (40x objective, 400x magnification, aperture 0.75). Photos were acquired with an Olympus DP21 camera and Olympus DP21-CB software (v. 02.01.01.93).

**FITC-dextran**

Mucosal integrity was assessed by measuring FITC-dextran intestinal permeability. For this, mice were fasted for 4h prior to 4kDa FITC-Dextran (0.4mg/g body weight) (Sigma-Aldrich, St. Louis, MO) oral gavage. Blood was collected 4hrs later and plasma FITC levels were determined using an Infinite M1000 PRO fluorescence spectrophotometer (Tecan) at 485 (excitation) and 535 nm (emission) along with a standard curve.

**Metabolic Analyses**

Animals were individually housed in a temperature controlled Promethion Metabolic Screening System (Sable Systems International, NV) where indirect calorimetry was performed to assess rates of oxygen consumption and carbon dioxide production. Food intake was acquired gravimetrically and ambulatory activity was acquired using a laser matrix. Mice were acclimated to this environment on a 12 hr light/dark cycle for 48 hr before the 24 hr recording period began. The respiratory exchange ratio (RER) was calculated as the ratio of carbon dioxide production to oxygen consumption, and energy expenditure was calculated using the Weir equation (Weir, 1949). Fecal bomb calorimetry was performed on feces collected during the 24 hour metabolic cage recording period, dehydrated in an oven at 60C for 48 hr, then combusted in technical duplicates with a Parr 6725 Semimicro Calorimeter to determine gross caloric density. When not analyzed in metabolic cages, food intake and fecal output were analyzed in cages holding 4-5 mice each and averaged per mouse. Food intake was analyzed by daily weighing of food and fecal output was assessed by collection in 2h-intervals.

**QUANTIFICATION AND STATISTICAL ANALYSIS**

Graphpad Prism software and R were used for graphical presentation and statistical calculations. Two-sided Mann-Whitney *U*-test was used to compare the means of two groups and two-sided Kruskal-Wallis *H*-test with Dunn's multiple comparisons test was used to compare the means of more than two groups. Pearson correlation was used to test correlation between two parameters and Log-rank test was used to compare survival between groups.  $p < 0.05$  was considered statistically significant and data are presented as mean  $\pm$  SEM. Number of biological replicates (*n*) and number of independent experiments are indicated in the figure legends.

**DATA AND SOFTWARE AVAILABILITY**

The accession number for the 16S rRNA sequencing data reported in this paper is ENA: PRJEB24887.

**Supplemental Information**

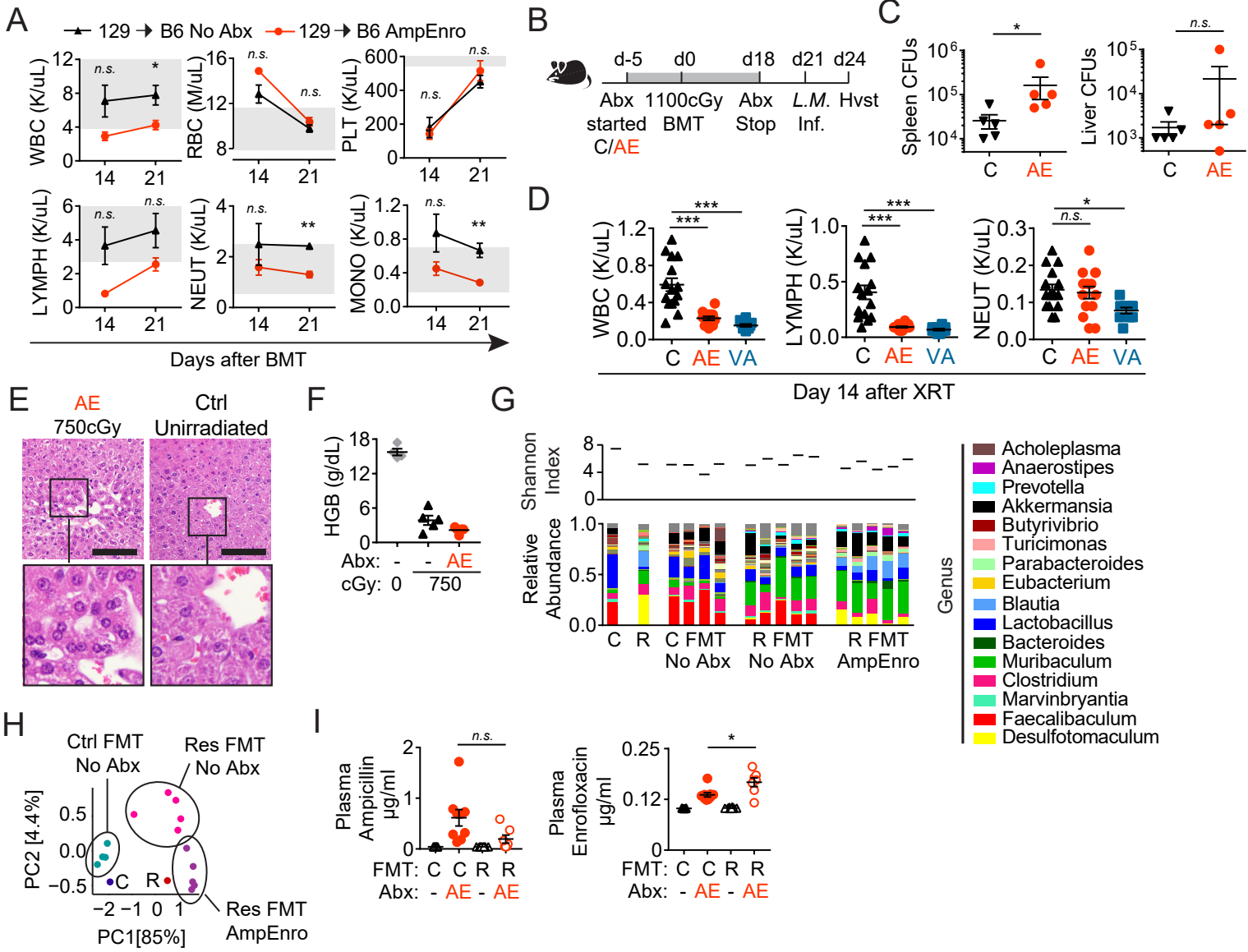
**Nutritional Support from the Intestinal Microbiota**

**Improves Hematopoietic Reconstitution**

**after Bone Marrow Transplantation in Mice**

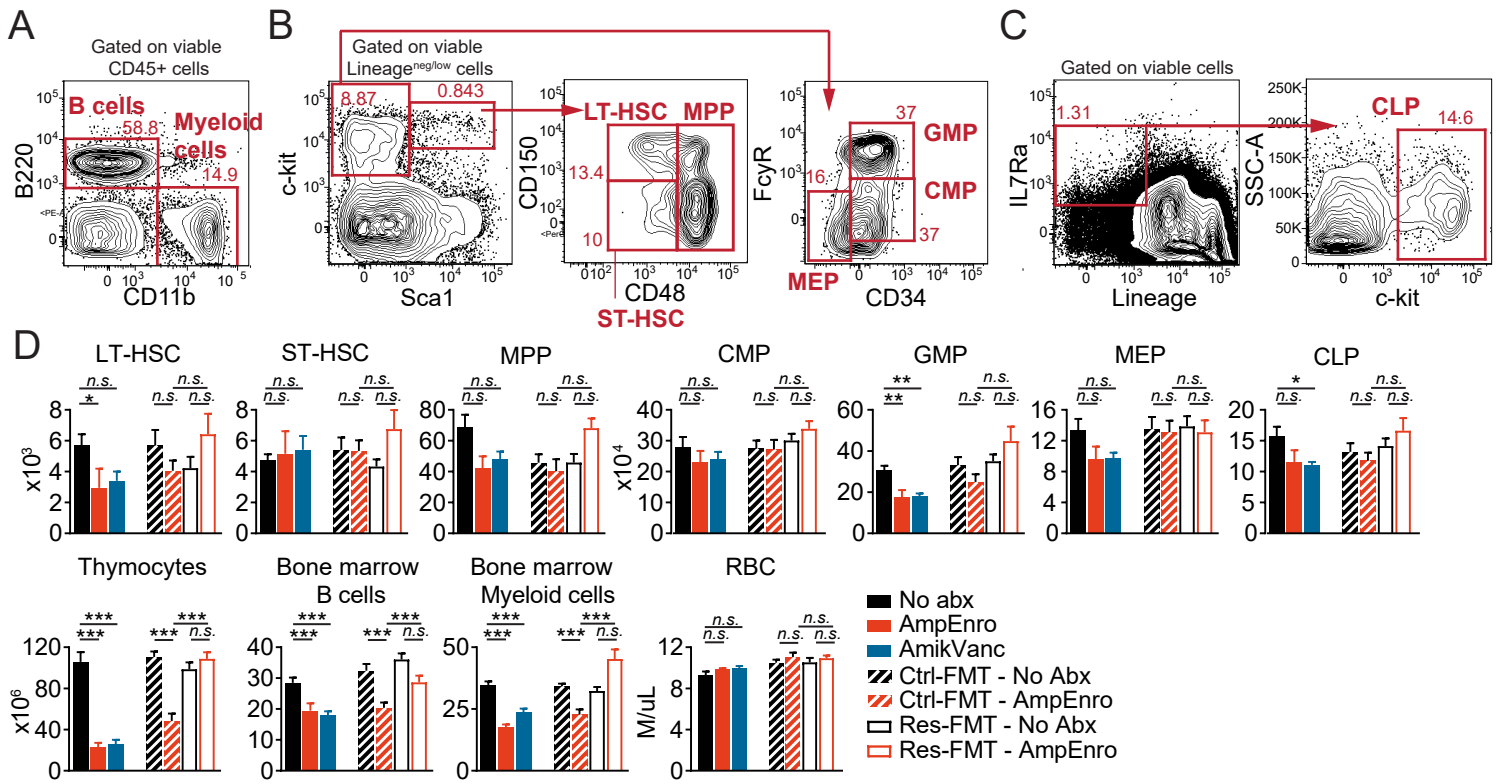
**Anna Staffas, Marina Burgos da Silva, Ann E. Slingerland, Amina Lazrak, Curtis J. Bare, Corey D. Holman, Melissa D. Docampo, Yusuke Shono, Benjamin Durham, Amanda J. Pickard, Justin R. Cross, Christoph Stein-Thoeringer, Enrico Velardi, Jennifer J. Tsai, Lorenz Jahn, Hillary Jay, Sophie Lieberman, Odette M. Smith, Eric G. Pamer, Jonathan U. Peled, David E. Cohen, Robert R. Jenq, and Marcel R.M. van den Brink**

Fig S1



**Related to Fig.1 (A)** WBC, RBC, PLT, LYMPH, NEUT, and MONO counts after BMT in C57BL/6J (B6) mice transplanted with 129S1/SvImJ (129) bone marrow cells without ( $n = 5$ ) and with ( $n = 4$ ) AE-treatment. Shaded areas indicate normal ranges. **(B)** Experimental outline for BMT and infection with *Listeria monocytogenes* (L.M.). **(C)** Quantification of viable bacteria in spleen and liver 3 days after infection in untreated mice ( $n = 5$ ) and AE-treated mice ( $n = 5$ ). **(D)** WBC, LYMPH, and NEUT counts 14 days after 750cGy irradiation in control mice ( $n = 15$ ), AE-treated mice ( $n = 15$ ), and VA-treated mice ( $n = 10$ ). **(E)** Representative images of hematoxylin- and eosin-stained liver sections centered around the central vein in moribund AE-treated mice 21 days after 750cGy radiation (left panels) and in age-matched untreated unirradiated control mice (right panels). Scale bar 100 $\mu$ m. **(F)** Hemoglobin concentration in untreated unirradiated mice ( $n = 4$ ) and untreated ( $n = 5$ ) and AE-treated ( $n = 5$ ) mice 21 days after 750cGy radiation. **(G)** Relative abundance at the genus level (lower panel) and Shannon diversity index (upper panel) in control- (C) and resistant- (R) FMT material and in untreated control FMT mice and resistant FMT mice without and with AE-treatment. **(H)** Principal components 1 and 2 based on weighted normalized UniFrac analysis of 16S Operational Taxonomic Unit (OTU) abundance. Numbers within brackets are percent variation explained by the component. **(I)** Quantification of ampicillin and enrofloxacin in plasma in mice given a control (C) FMT without ( $n = 9$ ) or with ( $n = 9$ ) AE-treatment and mice given a resistant (R) FMT without ( $n = 10$ ) or with ( $n = 7$ ) AE-treatment. Results except (A) and (C) represent at least two independent experiments. \*  $P < 0.05$ , \*\*  $P < 0.01$ , \*\*\*  $P < 0.001$ , n.s. – Not significant. Data is presented as mean  $\pm$  SEM.

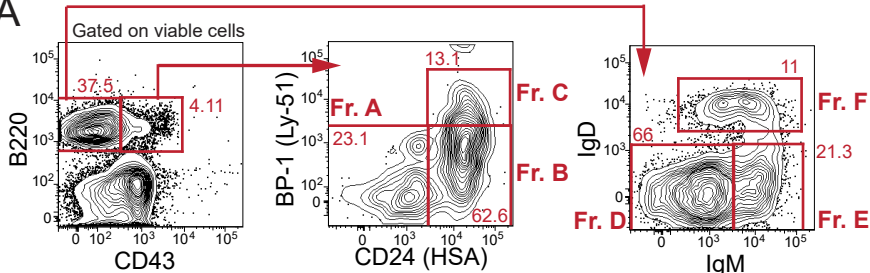
**Fig S2**



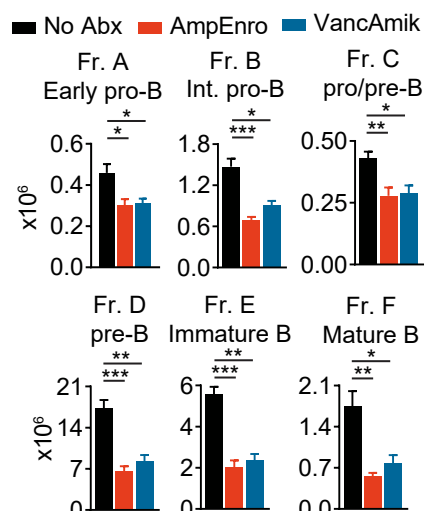
**Related to Fig 2.** **(A)** Gating of bone marrow B cells and myeloid cells. **(B)** Gating of hematopoietic stem cells, multipotent progenitors and myeloid progenitors. **(C)** Gating of common lymphoid progenitors. **(D)** Absolute counts of long-term hematopoietic stem cells (LT-HSC, Lin<sup>-</sup>Ckit<sup>+</sup>Sca1<sup>+</sup>CD150<sup>+</sup>CD48<sup>-</sup>), short-term hematopoietic stem cells (ST-HSC, Lin<sup>-</sup>Ckit<sup>+</sup>Sca1<sup>+</sup>CD150<sup>-</sup>CD48<sup>-</sup>), multi-potent progenitors (MPP, Lin<sup>-</sup>Ckit<sup>+</sup>Sca1<sup>+</sup>CD48<sup>+</sup>), common myeloid progenitors (CMP, Lin<sup>-</sup>Ckit<sup>+</sup>Sca1<sup>-</sup>FcγR<sup>low</sup>/<sup>-</sup>CD34<sup>+</sup>), granulocyte-monocyte progenitors (GMP, Lin<sup>-</sup>Ckit<sup>+</sup>Sca1<sup>-</sup>FcγR<sup>+</sup>CD34<sup>+</sup>), megakaryocyte-erythroid progenitors (MEP, Lin<sup>-</sup>Ckit<sup>+</sup>Sca1<sup>-</sup>FcγR<sup>-</sup>CD34<sup>-</sup>), common lymphoid progenitors (CLP, Lin<sup>-</sup>IL7Ra<sup>+</sup>Ckit<sup>+</sup>), thymocytes, bone marrow B cells and myeloid cells and peripheral red blood cells (RBC) in untreated ( $n = 10$ ), AE-treated ( $n = 8$ ), VA-treated ( $n = 10$ ), Ctrl-FMT mice without ( $n = 10$ ) or with AE treatment ( $n = 9$ ) and Res-FMT mice without ( $n = 10$ ) and with ( $n = 10$ ) AE-treatment 28 days after BMT. Results represent two independent experiments. \*  $P < 0.05$ , \*\*  $P < 0.01$ , \*\*\*  $P < 0.001$ , n.s. – Not significant. Data is presented as mean  $\pm$  SEM.

# Fig S3

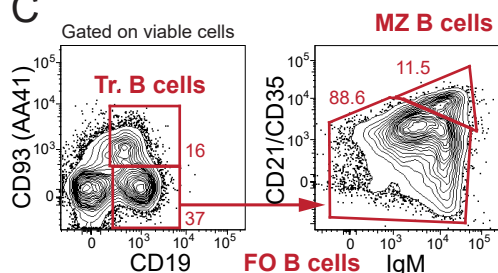
**A**



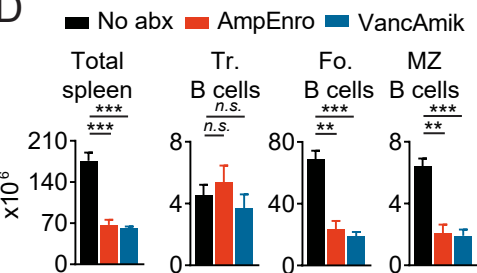
**B**



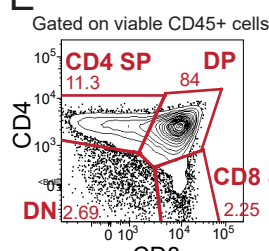
**C**



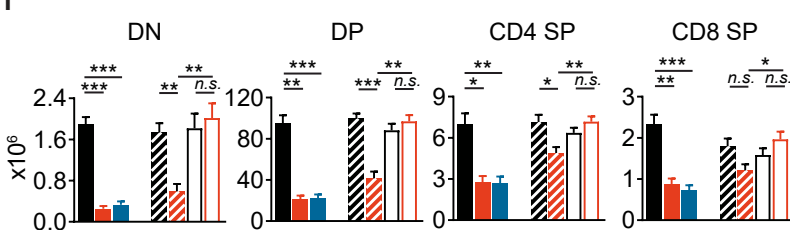
**D**



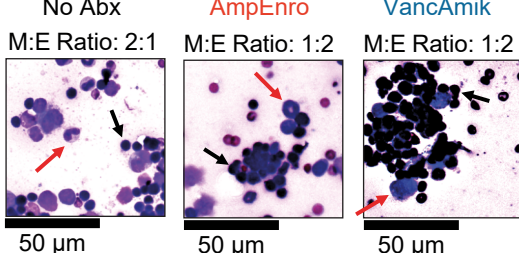
**E**



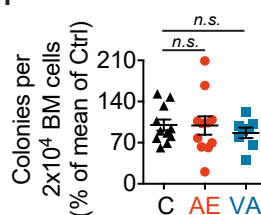
**F**



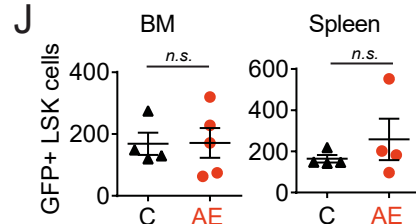
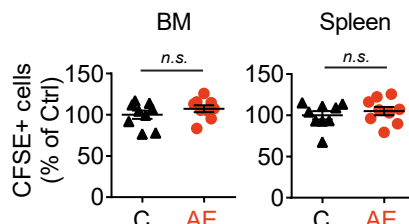
**G**



**H**

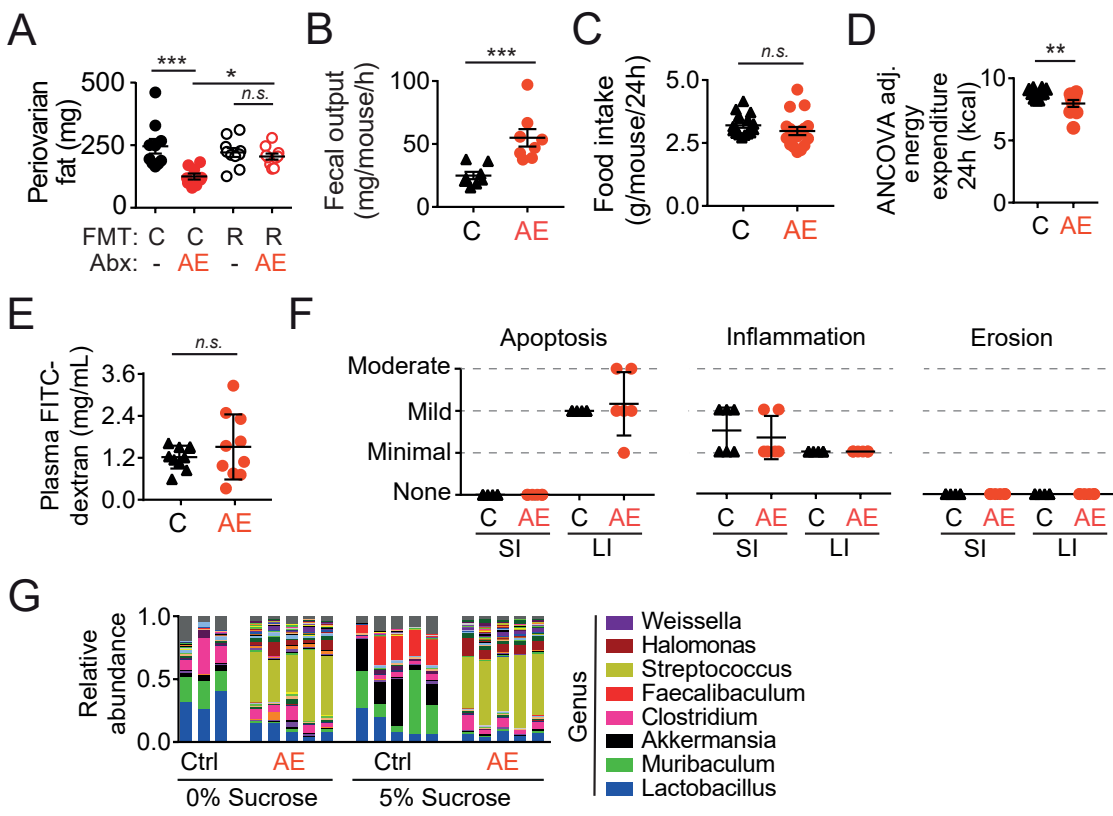


**I**



**Related to Fig. 2.** **(A)** Gating of bone marrow B cell subsets, **(B)** number of cells within B cell subsets in the bone marrow, **(C)** gating of splenic B cell subsets, and **(D)** number of cells within B cell subset in the spleen of untreated ( $n = 10$ ), AE-treated ( $n = 9$ ) and VA-treated mice ( $n = 10$ ) 28 days after BMT. Fr - fraction, Tr - transitional, FO - follicular, MZ - marginal zone. **(E)** Gating of thymic T cells and **(F)** number of cells within T cell subsets in the thymus of untreated mice ( $n = 10$ ), AE-treated ( $n = 8$ ), VA-treated ( $n = 10$ ), Ctrl-FMT mice without ( $n = 10$ ) and with AE treatment ( $n = 9$ ) and Res-FMT mice without ( $n = 10$ ) and with AE-treatment ( $n = 10$ ). DN – Double negative ( $CD4^-CD8^-$ ), DP – Double positive ( $CD4^+CD8^+$ ), and SP – Single positive ( $CD4^+CD8^-$  or  $CD4^-CD8^+$ ). **(G)** Representative photographs and assessment of myeloid to erythroid ratio (M:E) of Wright-Giemsa stained bone marrow brushings from untreated, AE- and VA-treated mice 28 days after BMT. **(H)** Number of myeloid colonies formed from  $2 \times 10^4$  bone marrow cells from untreated mice ( $n = 11$ ), AE-treated ( $n = 11$ ) and VA-treated mice ( $n = 8$ ) 28 days after BMT. **(I)** Number of CFSE+ cells in bone marrow and spleen 16h after injection of stained bone marrow cells ( $n = 10$  per group). **(J)** Number of GFP+ cells in bone marrow and spleen 16h after injection of GFP+ LSK cells in untreated mice and AE-treated mice ( $n = 5$  per group). Results except (J) represent at least two independent experiments. \*  $P < 0.05$ , \*\*  $P < 0.01$ , \*\*\*  $P < 0.001$ , n.s. – Not significant. Data is presented as mean  $\pm$  SEM.

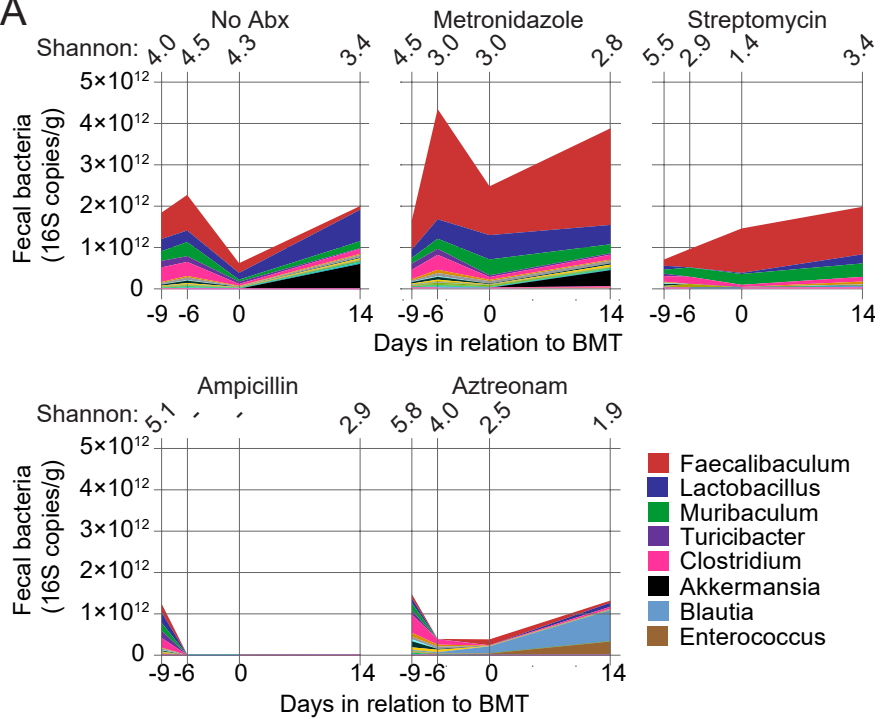
Fig S4



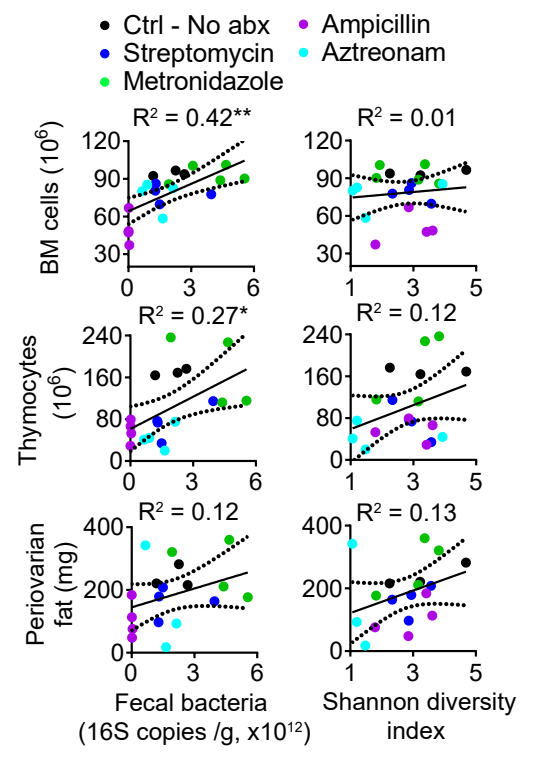
**Related to Fig. 3 and Fig. 4.** **(A)** Weight of periovarian fat 28 days after BMT in mice given a control FMT without ( $n = 10$ ) or with ( $n = 9$ ) AE-treatment and mice given a resistant FMT without ( $n = 10$ ) or with ( $n = 10$ ) AE-treatment. **(B)** Fecal output averaged per mouse in untreated and AE-treated mice post BMT ( $n = 8$  per group). **(C)** Food intake averaged per mouse in untreated and AE-treated mice post BMT ( $n = 11$  per group). **(D)** Total energy expenditure adjusted for lean mass using ANCOVA for untreated ( $n = 10$ ) and AE-treated ( $n = 10$ ) mice 13 days after BMT. **(E)** FITC-dextran concentration in plasma 4h after oral administration in untreated and AE-treated mice 21 days after BMT ( $n = 10$  per group). **(F)** Pathology scores of histology sections from small and large intestine in untreated and AE-treated mice 21 days after BMT ( $n = 6$  per group). **(G)** Relative abundance of bacterial genera in fecal samples 28 days after BMT in untreated and AE-treated mice with and without sucrose supplementation. Results represent at least two independent experiments. \*  $P < 0.05$ , \*\*  $P < 0.01$ , \*\*\*  $P < 0.001$ , n.s. – Not significant. Data is presented as mean  $\pm$  SEM.

# Fig S5

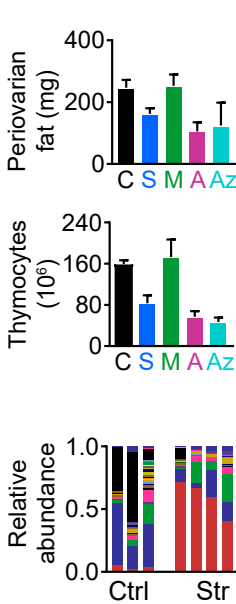
**A**



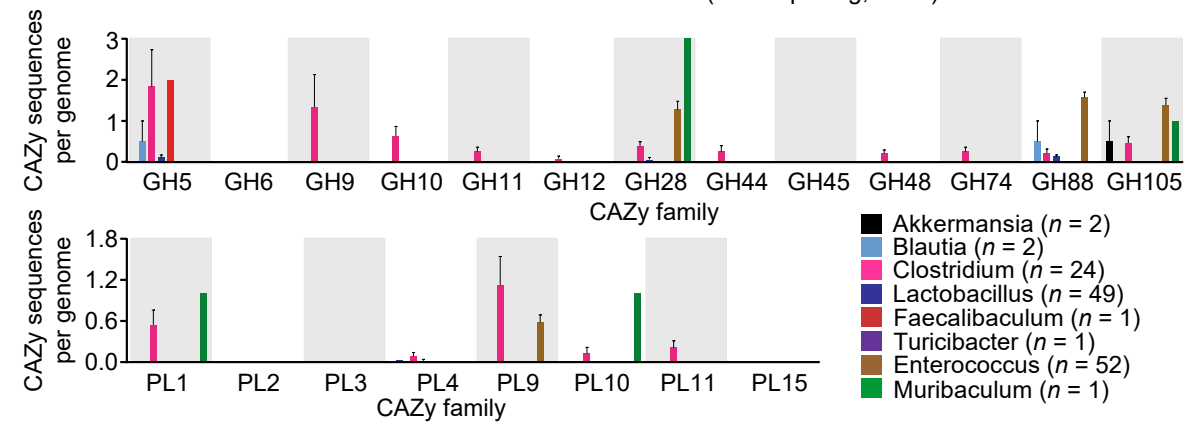
**B**



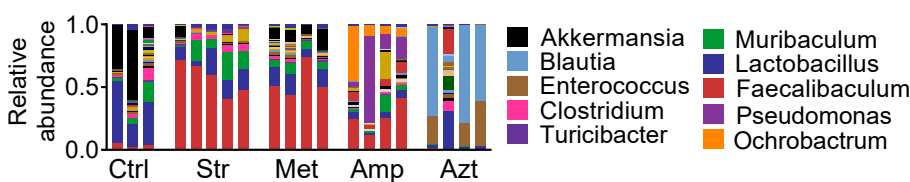
**C**



**D**

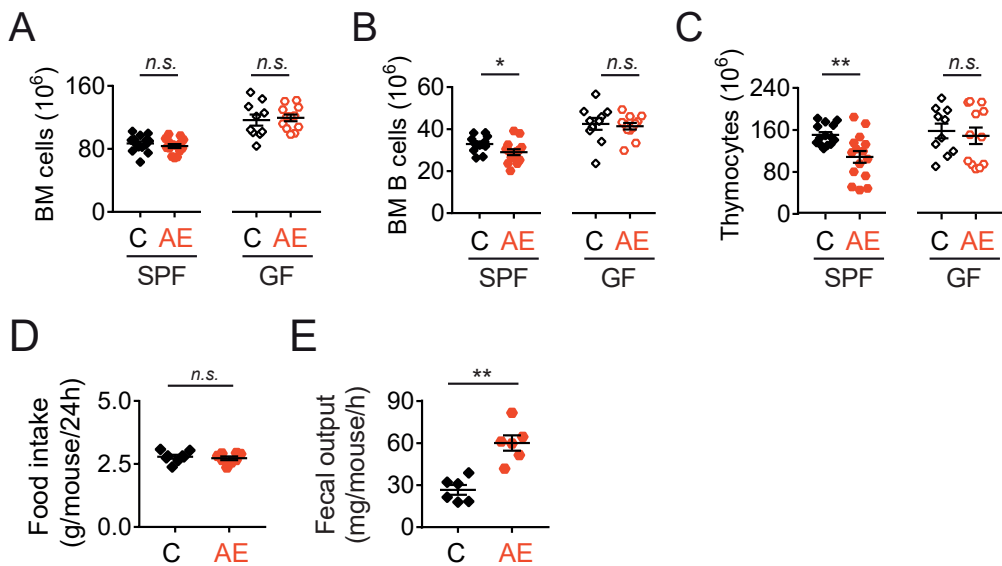


**E**



**Related to Fig. 5.** (A) Mean absolute bacterial abundance from start of treatment until 14 days after BMT based on 16S rRNA sequencing and qPCR. Untreated mice ( $n = 3$ ), mice treated with streptomycin ( $n = 4$ ), metronidazole ( $n = 5$ ), ampicillin ( $n = 4$ ), and aztreonam ( $n = 4$ ). (B) Pearson correlation of bone marrow cellularity, thymus cellularity and weight of peritoneal fat with bacterial load (16S rRNA copies) and Shannon diversity index 14 days after BMT in untreated mice (No abx,  $n = 3$ ) and mice treated with streptomycin ( $n = 4$ ), metronidazole ( $n = 5$ ), aztreonam ( $n = 4$ ), and ampicillin ( $n = 3$ ). (C) Peritoneal fat mass and number of thymocytes 28 days after BMT in untreated mice ( $n = 3$ ), and mice treated with streptomycin ( $n = 4$ ), metronidazole ( $n = 5$ ), aztreonam ( $n = 4$ ), and ampicillin ( $n = 3$ ). (D) To gain insight into the relative predicted ability of various microbiota genera to utilize complex carbohydrates, published genomes from the eight most common genera across the antibiotic-treated mice were scrutinized for sequences of enzymes classified into enzyme families known or predicted to participate in the digestion of the main dietary polysaccharides derived from plant cells (El Kaoutari et al., 2013) using the CAZy database ((Lombard et al., 2014), [www.cazy.org](http://www.cazy.org)). The number of analyzed genomes from each genus is indicated in the legend. (E) Relative abundance of bacterial genera in fecal samples 14 days after BMT in untreated mice, and mice treated with streptomycin (Str), metronidazole (Met), ampicillin (Amp), or aztreonam (Azt). \*  $P < 0.05$ , \*\*  $P < 0.01$ . Data is presented as mean  $\pm$  SEM.

**Fig S6**



**Related to Fig 6.** **(A)** Bone marrow cellularity, **(B)** number of bone marrow B cells ( $B220^+$ ), and **(C)** number of thymocytes in untreated specific pathogen free (SPF) mice ( $n = 14$ ), ampicillin (AE)-treated SPF mice ( $n = 15$ ), untreated germ-free (GF) mice ( $n = 10$ ) and AE-treated GF mice ( $n = 12$ ) after 35 days of antibiotic treatment. **(D)** Food intake averaged per mouse in untreated and AE-treated SPF mice ( $n = 8$  per group). **(E)** Fecal output averaged per mouse in untreated and AE-treated SPF mice ( $n = 6$  per group). Results represent at least two independent experiments. \*  $P < 0.05$ , \*\*  $P < 0.01$ , n.s. – Not significant. Data is presented as mean  $\pm$  SEM.